Ultrasound boosts doxorubicin efficacy against sensitive and resistant ovarian cancer cells

European Journal of Pharmaceutics and Biopharmaceutics 183 (2023) 119–131

Contents lists available at ScienceDirect

European Journal of Pharmaceutics and Biopharmaceutics

journal homepage: www.elsevier.com/locate/ejpb

Research paper

Ultrasound boosts doxorubicin efficacy against sensitive and resistant ovarian cancer cells

Federica Foglietta [a], Manuela Macrì [a], Patrizia Panzanelli [b], Andrea Francovich [c], Gianni Durando [d], Francesca Garello [e], Enzo Terreno [e], Loredana Serpe [a,*], Roberto Canaparo [a]

[a] Department of Drug Science and Technology, University of Torino, Via Pietro Giuria 13, 10125 Torino, Italy
[b] Department of Neuroscience Rita Levi Montalcini, University of Torino, Via Cherasco 15, 10126 Torino, Italy
[c] Institut de Physiologie, Université de Fribourg, Fribourg 1770, Switzerland
[d] National Institute of Metrological Research (INRIM), Strada delle Cacce 91, 10135 Torino, Italy
[e] Department of Molecular Biotechnology and Health Sciences, University of Torino, Via Nizza 52, 10126 Torino, Italy

ARTICLE INFO

Keywords:
Doxorubicin
Ultrasound
Sonodynamic therapy
Ovarian cancer
P-glycoprotein

ABSTRACT

Ovarian cancer (OC) is characterised by the highest mortality of all gynaecological malignancies, frequent relapses, and the development of resistance to drug therapy. Sonodynamic therapy (SDT) is an innovative anticancer approach that combines a chemical/drug (sonosensitizer) with low-intensity ultrasound (US), which are both harmless per sé, with the sonosensitizer being acoustically activated, thus yielding localized cytotoxicity often via reactive oxygen species (ROS) generation. Doxorubicin (Doxo) is a potent chemotherapeutic drug that has also been recommended as a first-line treatment against OC. This research work aims to investigate whether Doxo can be used at very low concentrations, in order to avoid its significant side effects, as a sonosensitiser under US exposure to promote cancer cell death in Doxo non-resistant (A2780/WT) and Doxo resistant (A2780/ADR) human OC cell lines. Moreover, since recurrence is an important issue in OC, we have also investigated whether the proposed SDT with Doxo induces immunogenic cell death (ICD) and thus hinders OC recurrence. Our results show that the sonodynamic anticancer approach with Doxo is effective in both A2780/WT and A2780/ADR cell lines, and that it proceeds via a ROS-dependent mechanism of action and immune sensitization that is based on the activation of the ICD pathway.

1. Introduction

Ovarian cancer (OC) represents the primary cause of death in gynaecological malignancies and the majority of women affected by OC are characterized by advanced disease stage at diagnosis and a five-year survival rate below 30 % [1,2]. A lack of symptoms and of specific screening, and the poor results obtained with standard treatments are the main reasons for this high mortality [3]. The available pharmacological approaches for OC, following surgery and according to stage and localisation, currently include a combination of conventional chemotherapeutic drugs, such as taxanes (*e.g.*, paclitaxel), carboplatin and gemcitabine [4]. In recent years, treatment strategies that make use of monoclonal antibody, such as bevacizumab, targeted drugs, such as poly (ADP-ribose) polymerase (PARP) inhibitors, and immunotherapy have been implemented [5,6]. However, OC treatment still presents many issues that have not yet been overcome, including the onset of drug resistance and relapse, which explain why overall mortality has changed very little over the last 30 years; ten-year survival remains poor, unlike other cancers in which reductions in mortality have been reported [7]. For this reason, a great deal of pharmacological research has been invested in improving OC treatment options and, of the conventional chemotherapeutic drugs available, considerable attention has been focused on the use of doxorubicin (Doxo) [8,9]. Doxo is a photosensitive anthracycline antibiotic that principally exerts anticancer activities by i) causing damage, at a nuclear level, by inhibiting both DNA replication and RNA transcription along with mitochondrial DNA replication, ii) provoking the inhibition of topoisomerase II activity, and iii) inducing free radial generation, leading to lipid peroxidation and direct membrane damage [10]. Doxo possesses strong anticancer cytotoxicity, but also has several side effects including haematological toxicity and progressive cardiac damage, while also inducing drug resistance [11,12]. The most important event in determining Doxo resistance is the

* Corresponding author at: Department of Drug Science and Technology, University of Torino, Via Pietro Giuria 13, 10125 Torino, Italy.
E-mail address: loredana.serpe@unito.it (L. Serpe).

https://doi.org/10.1016/j.ejpb.2023.01.005
Received 31 October 2022; Received in revised form 21 December 2022; Accepted 7 January 2023
Available online 9 January 2023

expression of ABC transporters, especially the P-glycoprotein (P-gp, ABCB1), that results in an increased drug efflux. The role of P-gp overexpression has been documented in different cancers where its expression is crucial for cancer cell survival and chemotherapy responsiveness as its overexpression elicits the development of the resistant phenotype [13,14].

One of the ways of attempting to treat advanced OC patients is therefore found in increasing Doxo efficacy, while, at the same time, abolishing its main drawbacks via the development, for example, of new formulations, such as pegylated liposomal formulations (PLD) [15–19]. Furthermore, several attempts to combine Doxo with photodynamic therapy (PDT) have also been made in order to increase free radical generation, as anthraquinones are common to provoke reactive oxygen species (ROS) and singlet oxygen ($^1O_2$) generation under light irradiation. However, Doxo's low quantum yield and its principally nuclear cellular localisation, which affect Doxo photoactivation, mean investigations have always included a photo-sensitiser agent that could provide a synergistic effect between PDT and low concentrations of Doxo [20–24]. While other strategies for improving the effectiveness and safety of Doxo in suppressing cancer growth while reducing its side effects and overcoming Doxo resistance have been investigated, the combination of Doxo with low intensity ultrasound (US) appears to be a promising strategy in this regard [25–28]. The main purpose of US is to increase Doxo uptake via the sonoporation mechanism. However, Fant and colleagues have recently investigated potentiating Doxo *in vitro* via US-induced non-inertial cavitation in a 4T1 murine mammary carcinoma cell line and have demonstrated significant reductions in cell viability and proliferation in their *in vitro* model, which rule out the influence of changes in Doxo uptake on treatment outcome [29–32]. This finding sheds new light on the different roles that Doxo may play under US irradiation, and hints at a possible application of Doxo as a sonosensitiser in sonodynamic therapy (SDT). SDT is a revolutionary non-invasive anticancer strategy that combines US and a chemical/drug (named a sonosensitiser) that only exerts a therapeutic effect upon US activation, generating oxidative damage followed by cancer cell death [33]. The components, the sensitiser and US, should be harmless per se, and only lead to cytotoxic events when combined [34]. It is thought that sonosensitiser activation is triggered by US-induced acoustic cavitation [33], and, more specifically, it has been suggested that US-induced acoustic cavitation can lead to sonoluminescence, which may be responsible for sonosensitiser activation and the subsequent production of highly toxic ROS [35,36]. Another intriguing hypothesis for sonosensitiser activation via US suggests that membranes are able to transform the oscillating US acoustic pressure wave into intra-membrane cavitation under suitable conditions, releasing considerable energy that can, in our opinion, trigger sonosensitiser activation and subsequent ROS production [37].

SDT offers many potential and significant advantages, such as i) non-invasively eradicating solid tumours in a site-directed manner, ii) overcoming Doxo resistance, iii) preventing the significant side effects of Doxo, as it can be used at harmless concentrations per sé and iv) eliciting antitumor immunity responses via the induction of immunogenic cell death (ICD) [38–40]. In our opinion, these characteristics might significantly improve treatment outcomes in Doxo resistant and non-resistant OC. This research work therefore aims to investigate whether Doxo, used at concentrations that are otherwise non-cytotoxic, may act as a sonosensitiser under US exposure, and thus promote cancer cell death in human Doxo non-resistant (A2780/WT) and Doxo resistant (A2780/ADR) OC cell lines. In this regard, the anticancer activity induced by Doxo after US exposure on the A2780/WT and A2780/ADR cells has been investigated in terms of cytotoxicity, ROS production, cell cycle distribution, DNA damage, mitochondrial membrane potential, lipid peroxidation and cell death mechanisms. Finally, as the SDT approach investigated in this work has been suggested as a potential front-line treatment against OC, we have investigated whether SDT can act as an ICD inducer with the aim of avoiding OC recurrence.

2. Materials and methods

2.1. Cell culture

Two different human cell lines, Doxo non-resistant (A2780/WT, ECACC 93112519) and Doxo resistant (A2780/ADR, ECACC 93112520) ovarian carcinoma, were acquired from the European Collection of Authenticated Cell Cultures (ECACC, UK) and were established from an ovarian endometroid adenocarcinoma of an untreated patient. A2780/WT cells were maintained as monolayers in Doxo-free complete medium made of RPMI 1640 medium enriched with foetal calf serum (10 %, v/v), streptomycin (100 μg/ml) and penicillin (100 units/ml), L-glutamine (2 mM) (Sigma-Aldrich, Milano, Italy). The A2780/ADR cells were maintained in culture with complete medium with the addition of Doxo 10^{-7} M, following manufacturer's instructions. Both the cell lines considered were maintained in culture in an incubator for a maximum of 10 passages at 37 °C in a humidified atmosphere with 5 % CO_2 and then discarded. Moreover, the A2780/ADR cells were periodically tested with calcein-AM (Sigma-Aldrich, Milano, Italy), a substrate of P-glycoprotein (P-gp), by cytofluorimetric evaluation to assess Doxo resistance over time.

2.2. IC_{50} calculation and doxorubicin cell cytotoxicity assay

Doxorubicin hydrochloride was purchased as a powder (Sigma-Aldrich, Milano, Italy) with a molecular weight of 579.98 g/mol, was resuspended in DMSO at a concentration of 14 mM and then aliquoted to small volumes (100 μL) for storage at −20 °C. RPMI 1640 complete medium was used to obtain the proper dilution concentration from the 14 mM Doxo solution. In order to assay cytotoxicity and to calculate IC_{50} after Doxo incubation, 1.5×10^3 cells were seeded in 96-well culture plates (Techno Plastic Products, Switzerland) in 100 μL of culture medium in replicates (n = 8) and then incubated with increasing concentrations of Doxo (0.00001, 0.0001, 0.001, 0.01, 0.1, 1, 10 and 100 μM). The assay was performed on both A2780/WT and A2780/ADR cell lines. WST-1 assay (Roche Applied, Basel, Switzerland) was used to assess cell proliferation with the WST-1 reagent (10 μL) being added in the three time points (24, 48, and 72 h) and incubated for 2 h at + 37 °C. The absorbance of the well (abs) was determined at 450 nm and 620 nm was used as reference wavelength in a microplate reader (Asys UV340; Biochrom, UK). Cytotoxicity was displayed as a percentage in agreement with the equation: % cytotoxicity = $100 \times (abs_{control} - abs_{sample})$. It was also verified that the highest concentration of DMSO (0.7 %) in the wells, corresponding to 100 μM doxorubicin, didn't cause any toxicity. Finally, the calculation of doxorubicin IC_{50} was performed using CalcuSyn software (Biosoft, Cambridge, UK, version 2.0).

2.3. In vitro sonodynamic treatment

Doxo was used for SDT at non-cytotoxic concentrations, which were obtained from the cytotoxicity assay, to act solely as a sonosensitiser. Specifically, Doxo was used at 0.05 μM after 24 h incubation in A2780/WT and at 0.50 μM after 1 h incubation in A2780/ADR. The Doxo-enriched medium was removed before SDT. After Doxo incubation in the sonodynamic experiments, cells were harvested, counted and then normalised to 5×10^5 cells in a polystyrene tube filled with 2.5 mL of PBS at pH 7.4. The *in vitro* sonodynamic experiments were carried out in the dark and, to avoid hyperthermia during the experiment, the temperature of the medium was always controlled. A plane wave transducer (with a diameter of 2.5 cm) was used to generate US, operating in pulsed mode (50 %, duty cycle, DC) at a frequency of 1.866 MHz, that was combined to a power amplifier (Type AR 100A250A; Amplifier Research, Souderton, USA) and a function generator (Type 33250; Agilent, USA). A custom-built mechanical adaptor was filled with ultrapure water and attached to the 1 cm diameter polystyrene tube, where cell suspension was introduced (Fig. 1). An US power of 2 W/cm^2,

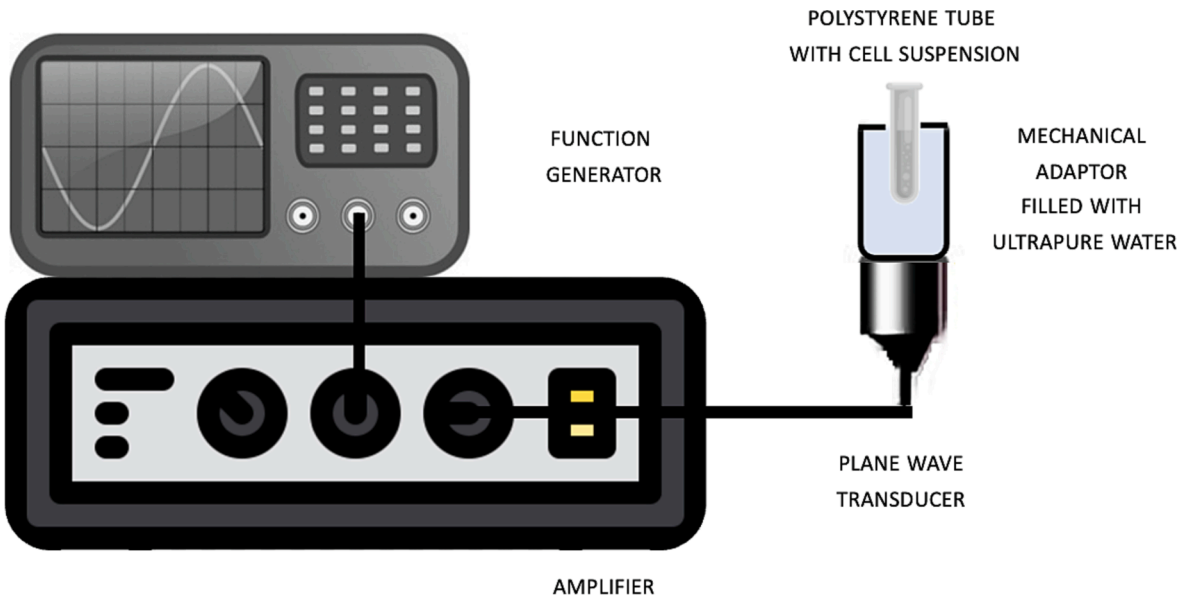

Fig. 1. Schematic representation of the set-up for the *in vitro* ultrasound treatments.

50 % DC,50 % DC, for a total of 5 min was used as experimental condition, under subdued light. After SDT, 2.5×10^3 cells were seeded in 100 μL of culture medium in 96-well culture plates in replicates (n = 8). The WST-1 assay was then carried out to investigate the effects of treatment on cell proliferation, and results shown as a percentage with respect to control cells (untreated cells).

2.4. Fluorescence and confocal microscopy

Fluorescence and confocal microscopy were used to investigate the localisation of Doxo within the A2780/WT and A2780/ADR cells, in order to furnish qualitative evidence for intracellular localisation at the time of US exposure. Briefly, 1×10^5 A2780/WT and A2780/ADR cells were seeded on glass coverslips in 24-well plates and were then treated with Doxo for 24 h at 0.05 μM and for 1 h at 0.50 μM, respectively. When the incubation ended, the slides were washed with PBS and then underwent to a fixation for 15 min with 4 % paraformaldehyde (Sigma-Aldrich, Milano, Italy). An incubation with 4′,6-diamidin-2-fenilindol (DAPI) for 15 min was used to stain cell nuclei. Finally, fluorescence images were collected using a DMI4000B fluorescence microscope with an LAS acquisition system (Leica, Wetzlar, Germany, version 3.8.0) and photographed at 40x magnification with an oil-immersion objective. In order to thoroughly investigate the Doxo accumulation inside the cells, confocal images were also obtained using a confocal microscope (Zeiss LSM5 Pascal, Oberkochen, Germany) with a laser scanning (λ_{ex} 405 nm diode laser, λ_{em} 633 nm) and with a 40x oil-immersion objective in multi-track mode. ImageJ (Fiji, Bristol, UK, version 2.0) was used to process all the imagines.

2.5. Flow cytometry

Flow cytometric assays were carried out to investigate the cellular uptake of Doxo, ROS generation, mitochondrial-membrane potential, sonoporation occurrence, cell-death type, cell-cycle distribution as well as calreticulin (CRT) and high mobility group box 1 (HMGB1) cell-surface expression after the various treatments. Furthermore, the ability of the A2780/ADR cell line to maintain resistance to Doxo was evaluated via flow cytometry. All of the aforementioned assays were assessed using a C6 flow cytometer (Accuri Cytometers, Annarbor, MI, USA), with 10,000 events being considered for the analysis at a medium flow rate and by discharging cellular debris. Firstly, the cellular uptake of Doxo was evaluated according to its intracellular fluorescence in a flow cytometric analysis at 488 nm excitation (λ_{ex} 488 nm, $\lambda_{em} > 670$ nm), after the A2780/WT and A2780/ADR cells were exposed for 1, 3, 6, 12 and 24 h to both 0.05 and 0.50 μM Doxo. Cellular uptake was expressed as the integrated mean fluorescence intensity (iMFI), which represents the product of the frequency of Doxo positive cells and the mean fluorescence intensity of the cells.

SDT-induced intracellular ROS production was assessed using 2,7-dichlorofluorescein diacetate (DCFH-DA, Molecular Probes, USA) as the intracellular probe to investigate the oxidative stress in both cell lines. Briefly, 10 μM DCFH-DA was incubated with cells for 30 min at the end of Doxo incubation. Then, the cells were washed with PBS, trypsinised, normalised to 5×10^5 cells, collected in 2.5 mL of PBS and treated with US. The production of ROS was measured 1, 5, 10, 15, 30 and 60 min after treatment and expressed as iMFI ratio in order to get information on the ratiometric variation in fluorescence per time point with respect to control cells (untreated cells). This ratio represented the difference in the iMFI of treated and untreated cells over the iMFI of untreated cells [41]. When the iMFI ratio started to decrease, due to the significant increase in DCF fluorescence in control cells, ROS detection was stopped, to avoid any assay artefacts that may interfere with evaluations of the real intracellular ROS content induced by the considered treatments.

The mitochondrial-membrane potential (Δψm) was determined 1 h after the treatment in the A2780/WT and A2780/ADR cells using the BDTM Mitoscreen kit (BD Bio-sciences, San Jose, CA, USA), which is based on the cation dye 5,5,6,6-tetrachloro-1,1,3,3-tetraethylbenzimidazolylcarbocyanine iodide (JC-1), following manufacturer's instructions. In a few words, JC-1 is a double fluorescent stain of mitochondria that can either be observed as green fluorescent monomers or as red fluorescent aggregates, and that is used to monitor Δψm because it does not accumulate in mitochondria with depolarised $\Delta_{\psi m}$ and remains in the cytoplasm as monomers. Cytometric data are expressed as the aggregate/monomer ratio. Moreover, a positive control was carried out in the assay by incubating cells with 500 μM hydrogen peroxide (H_2O_2) for a total of 3 h. The occurrence of cytoplasmic membrane sonoporation in the A2780/WT and in the A2780/ADR cells was investigated using calcein-AM and propidium iodide (PI) after US exposure to perform SDT in order to distinguish viable sonoporated cells from non-sonoporated cells and dead cells. Cells at subconfluence were trypsinised and collected in a polystyrene tube at a concentration of $5x10^5$. 1 μL of PI (10 μg/mL) was added to the tube, SDT (described above) was performed and then 2 μL of calcein-AM was added. Cells

were put in incubation for 15 min at 37 °C and events were then acquired by flow cytometry.

Cell death after SDT in both cell lines was obtained using the Dead Cell Apoptosis kit, which is based on Sytox® Green and allophycocyanin (APC)-Annexin V (Life Technologies, Milano, Italy), in accordance with manufacturer's instructions. Briefly, $5x10^5$ A2780/WT and A2780/ADR cells were treated with US (2 W/cm^2, 1.866 MHz, DC 50 % for 5 min) after Doxo incubation at 0.05 μM and 0.50 μM, respectively, and seeded in culture flasks. Thirty-six h after treatment, cells were trypsinized, collected in polystyrene tubes and then stained with APC-Annexin V and Sytox® Green. The samples were acquired on a flow cytometer to measure APC-Annexin V (λ_{ex} 640 nm, λ_{em} 675/25 nm) and Sytox® Green (λ_{ex} 488 nm, λ_{em} 533/30 nm), and any cell debris with low side light scatter (SSC) and low forward light scatter (FSC) were dismissed from the analyses. A total of 10,000 events were examined for APC-Annexin V and Sytox® Green staining to discriminate from viable cells (negative to APC-Annexin V and to Sytox® Green), late apoptotic/necrotic cells (positive to APC-Annexin V and to Sytox® Green) and apoptotic (positive to APC-Annexin V). All analyses were performed using the FCS Express software (BD Bioscience, San Jose, CA, USA, version 4.0). The cell-cycle distribution of A2780/WT and A2780/ADR cells after SDT was evaluated using Vybrant® cell dye (Life Technologies, Italy) 36 h after treatment, in agreement with the manufacturer's instructions, and the FCS Express software (BD Bio-science, San Jose, CA, USA, version 4.0).

The cell-surface exposure of CRT, as a damage associated molecular pattern (DAMP), was determined 48 h after SDT. Briefly, A2780/WT cells were washed with PBS, trypsinised and then incubated for 40 min at room temperature with Alexa Fluor® 488 anti-calreticulin antibody (ab196158, Abcam, Cambridge, UK) at 10 μg/mL, under cover from light. When the incubation finished, cells were washed twice with PBS and then analysed by a C6 flow cytometer, at 488 nm excitation (λ_{ex} 488 nm, λ_{em} 530 nm). 1×10^4 events were considered in the analysis at a medium flow rate and by discarding cellular debris. The occurrence of HMGB1 as a DAMP was determined 48 h after SDT. A2780/WT cells were washed with PBS, trypsinized and incubated for 30 min at room temperature with anti-HMGB1 antibody (ab77302, Abcam, Cambridge, UK) at 10 μg/mL, under cover from light. When the incubation finished, cells were washed once with PBS and then incubated for 1 h at room temperature with rabbit F(ab')2 anti-mouse IgG H&L (Alexa Fluor® 488) (ab169345, Abcam, Cambridge, UK) at 1:2000, under cover from light. When the incubation ended, cells were washed twice with PBS and then analysed by the C6 flow cytometer, at 488 nm excitation (λ_{ex} 488 nm, λ_{em} 530 nm). 1×10^4 events were considered in the analysis at a medium flow rate, discarding cellular debris. Finally, the ability of the A2780/ADR cell line to maintain its resistance to Doxo was regularly evaluated cytofluorimetrically using a calcein-AM assay in order to assess the functioning of P-gp activity, which is responsible for the Doxo-resistant phenotype in the A2780/ADR cell line [42]. Briefly, detached cells were incubated with calcein AM (2 mM in DMSO) incubated at 37 °C for 15 min.

2.6. Gene expression analysis

To investigate the SDT effect with Doxo on mRNA gene expression, total RNA was isolated from A2780/WT and A2780/ADR cells 24 h after treatment. Briefly, 1.0 x 10^5 cells were considered and stored at −80 °C in RNA Cell Protection Reagent (Qiagen, Milano, Italy). The RNeasy Plus Mini kit (Qiagen, Italy) was used to determine the Total RNA and a Qubit fluorometer (Life Technologies, Milano, Italy) was used to obtain the total RNA concentration (μg/mL). To carry out real-time (RT-PCR) analysis, the QuantiTect Reverse Transcription kit (Qiagen, Milano, Italy) was used to reverse transcribe 150 ng of total RNA into 20 μL cDNA reaction volume. Then, 10 μL real time RT-PCR reaction were considered that contained 12.5 ng of cDNA, according to manufacturer's instructions. The SsoFast EvaGreen (Bio-Rad, Hercules, CA, USA) was used to perform quantitative RT-PCR, and the QuantiTect Primer Assay (Qiagen, Milano, Italy), *CDK1* (QT00042672), *CDKN1A* (QT00062090) and *TP53* (QT00060235), were then considered. To normalise mRNA data, the transcript of the reference 18S ribosomal RNA (*RRN18S*, QT00199367) was used, and real-time PCR was performed using a MiniOpticon Real Time PCR system (Bio-Rad, Hercules, CA, USA). The PCR protocol conditions considered were as follows: a Taq DNA polymerase activation step at 95 °C for 30 *sec*, followed by 40 cycles at 95 °C for 5 *sec* and 55 °C for 10 *sec*. At least three independent cDNA preparations per sample were carried out for all runs and all samples were run in duplicate, including two non-template controls in all PCR runs. Data analysis was determined by using the Bio-Rad CFX manager software (Bio-Rad, Hercules, CA, USA, version 3.1), following the manufacturer's instructions. All analyses were completed in compliance with Minimum Information for Publication of Quantitative Realtime PCR Experiment (MIQE) guidelines [43].

2.7. Lipid peroxidation assay

Changes in lipid peroxidation levels in the A2780/WT and A2780/ADR cells 36 h after SDT were determined using the Lipid Peroxidation Assay kit (Abcam, Cambridge, UK) to detect the malondialdehyde (MDA), which is produced as an end product of lipid peroxidation. Free MDA present in the samples reacts with thiobarbituric acid (TBA) and produces the MDA-TBA adduct, quantified via colorimetric detection at 540 nm with a microplate reader (Bio-Rad, Hercules, CA, USA). Analysis was performed following the manufacturer's instructions and the data, after the standard curve was plotted, are expressed as nmol of detected MDA.

2.8. Analysis of DNA damage

DNA damage was measured 36 h after the SDT of A2780/WT and A2780/ADR cells using the DNA damage-AP site-Assay kit (Abcam, Cambridge, UK), following the manufacturer's instructions, on extracted DNA from control and treated samples. The assay provides a specific colorimetric method for the detection of the formation of apurinic/apyrimidinic sites (AP sites), which represent one of the major DNA lesions [44]. A biotinylated aldehyde reactive probe (ARP) reagent (N9-aminooxymethylcarbonylhydrazinoD-biotin) is used in the assay that specifically reacts with the aldehyde group on the open ring of the AP sites. Biotin residues, used to tag the AP sites, are later quantified using the streptavidin-enzyme conjugate, detected then at 450 nm on a microplate reader (Bio-Rad, Hercules, CA, USA) upon the removal of background signals. DNA damage is expressed as the ratio between the number of AP sites in 100,000 bp in treated and untreated cells.

2.9. ATP assay

ATP quantification after SDT was detected using the ATP assay kit (Abcam, Cambridge, UK), in accordance with the manufacturer's instructions. This ATP assay relies on glycerol phosphorylation, which forms a product that can be detected using colorimetric techniques. In this way, it is possible to quantify total ATP in cellular lysates. The ATP assay was performed 24 h after SDT when cells were preincubated with Doxo 0.05 μM for 24 h. Briefly, 5.0×10^5 cells were considered for each experimental condition, detached from the flasks and then lysated. At the end of the assay, ATP was otained by reading well absorbance on a microplate reader (Bio-Rad, Hercules, CA, USA) at λ_{ex} 535/λ_{em} 587 nm. ATP concentration expressed as nmol/μL was then calculated using an ATP standard curve.

2.10. Statistical analysis

Statistical analyses were carried out with Prism software (GraphPad, La Jolla, CA, USA, version 9.0). Data are presented as mean values ±

standard deviation of three independent experiments. One-way ANOVA, two-way ANOVA and multiple *t*-test analysis of variance and, to calculate the threshold of significance, Bonferroni's test was used, according to the design of the experiment. The statistical significance threshold was set at $p \leq 0.05$.

3. Results

3.1. Doxorubicin IC_{50} and cellular uptake in A2780/WT and A2780/ADR cells

A2780/WT and A2780/ADR cells were first incubated with increasing Doxo concentrations over time in order to determine the maximum non-cytotoxic concentration that could be used to perform the sonodynamic experiments. By observing Fig. 2 (A,B), we can appreciate that a concentration of 0.1 μM was able to induce slight cytotoxicity in A2780/WT cells as soon as 24 h after Doxo incubation, while, in A2780/ADR cells, the Doxo-resistant cell line, increased cytotoxicity was only observed 24 h after incubation at the highest Doxo concentration, 100 μM. The data obtained from the cytotoxicity curves were used to calculate the IC_{50} through CalcuSyn software for both cell lines. For A2780/WT cells, an IC_{50} of 1.66 ± 0.19 μM at 24 h, an IC_{50} of 0.70 ± 0.16 μM at 48 h and an IC_{50} of 0.22 ± 0.02 μM at 72 h were obtained. On the other hand, an IC_{50} of above 100.00 μM was estimated for all of the three investigated times for A2780/ADR cells. By taking these data into consideration, it was decided that the experiments would be carried out on A2780/WT and A2780/ADR cells at non-cytotoxic Doxo concentrations; concentrations lower than the IC_{05} (drug concentration needed to inhibit 5 % of cell growth), which were calculated to be Doxo 0.05 μM and 0.5 μM, for A2780/WT and A2780/ADR cells, respectively.

The ability of both cell lines to internalise Doxo was evaluated by flow cytometry thanks to Doxo's fluorescence properties. Specifically, the values of the product of the frequency of Doxo-positive cells and the cell mean fluorescence intensity (iMFI) were determined over time. For this analysis, both concentrations of interest - 0.05 μM and 0.50 μM - were investigated in A2780/WT (Fig. 2C) and A2780/ADR (Fig. 2D) cells in order to highlight the differences in Doxo-cell. As shown in Fig. 2C, concentration- and time-dependent increases in iMFI values were observed in A2780/WT cells, while in A2780/ADR cells it was only possible to observe only a slight time-independent increase in iMFI values at 0.50 μM Doxo. As expected, the activity of P-gp, which was monitored using the calcein-AM flow cytometric assay, was found to be very low in the non-resistant cell line and very high in the resistant cell line, (Fig. 2E).

3.2. Evaluation of sonodynamic activity of doxorubicin

Based on the data obtained from the above-mentioned cytotoxicity and cellular uptake studies above-mentioned, the concentrations and incubation times for Doxo to act as a sonosensitiser were set at 0.05 μM for 24 h in A2780/WT cells and 0.50 μM for 1 h in A2780/ADR cells. The A2780/WT and A2780/ADR cells were incubated with Doxo 0.05 μM for 24 h and 0.50 μM for 1 h, then underwent to US exposure and cell proliferation was finally examined up to 72 h after treatment. A statistically significant reduction in cell proliferation was observed in A2780/WT cells after SDT at 48 h ($p \leq 0.01$) and at 72 h ($p \leq 0.001$), compared to untreated cells, while no significant decrease in cell proliferation was noticed when cells were exposed to Doxo and US separately, compared to untreated cells (Fig. 3A). It is worth nothing that similar effects on cell proliferation were also noticed after each set of treatment conditions in A27880/ADR cells (Fig. 3B). Sonodynamic experiments were all executed on A2780/WT and A2780/ADR cells with the Doxo incubation time before US exposure being changed in order to evaluate whether responsiveness to treatment changed compared to the previously reported experimental conditions. In particular, A2780/WT cells underwent to 0.05 μM Doxo exposure for 1 h before SDT, whereas A2780/ADR cells were exposed to 0.50 μM Doxo for 24 h before SDT. No statistically significant differences in cell proliferation were noticed in both the cell

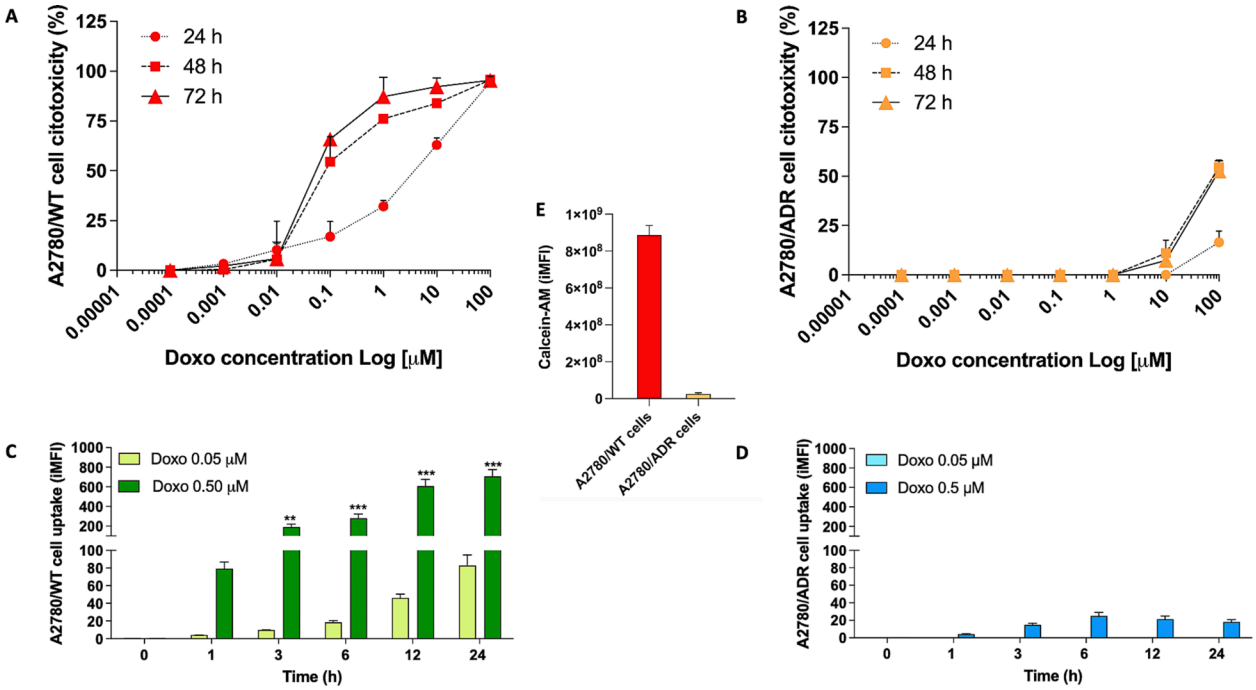

Fig. 2. Doxo cytotoxicity, uptake and P-gp activity in A2780/WT and A2780/ADR cells. Different Doxo concentrations (0.00001, 0.0001, 0.001, 0.01, 0.1, 1, 10 and 100 μM) were considered to incubate A2780/WT (A) and A2780/ADR (B) cells, and cytotoxicity was calculated using a WST-1 cell proliferation assay at 24, 48 and 72 h. Cells were then incubated with Doxo 0.05 and 0.50 μM, and cellular uptake was evaluated at different time points (1, 3, 6, 12 and 24 h) using flow cytometry on both A2780/WT (C) and A2780/ADR (D) cells. The iMFI values of calcein-AM, a substrate of P-gp, shows P-gp activity in both cell lines (E). Data are shown as mean ± standard deviation (n = 3). Statistical significance of Doxo 0.5 μM *versus* Doxo 0.05 μM, ** $p \leq 0.01$ and *** $p \leq 0.001$.

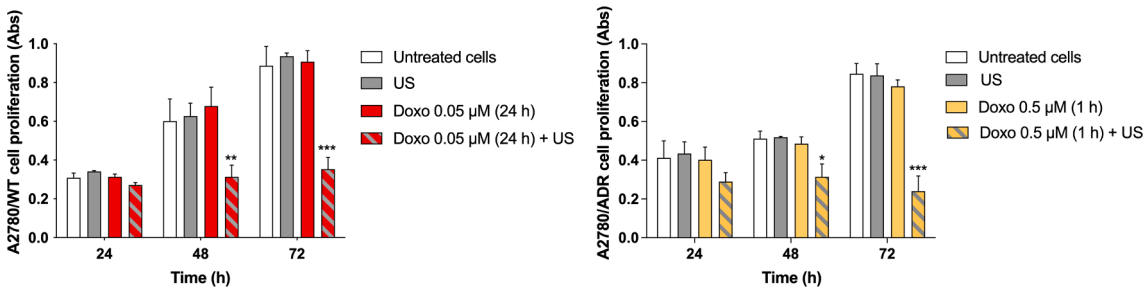

Fig. 3. Effect of SDT with Doxo on A2780/WT and A2780/ADR cells. Cells were pre-incubated with Doxo (0.05 μM for 24 h in A2780/WT and 0.50 μM for 1 in A2780/ADR) and then underwent to US exposure (2.0 W/cm^2 at 1.866 MHz, 50 % DC, for 5 min). Cell proliferation was performed at 24, 48 and 72 h in a WST-1 assay. Statistical significance *versus* untreated cells: * $p \leq 0.05$, ** $p \leq 0.01$, *** $p \leq 0.001$.

lines after each treatment (data not shown). The different outcomes observed, compared to the previous treatments, can be ascribed, in A2780/WT cells, to Doxo concentration-dependent responsiveness as the amount of intracellular Doxo after 1 h of incubation is significantly lower than that after 24 h incubation (Fig. 2C). On the other hand, the inefficacy of treatment in A2780/ADR cells can be ascribed to Doxo time-dependent responsiveness caused by the different localisation of Doxo, perhaps because of P-gp activity.

3.3. ROS production induced by sonodynamic activation of doxorubicin

Doxo's ability to produce ROS is one of its principal actions inside cells [45]. We therefore decided to analyse, using flow cytometry, ROS production after SDT with Doxo. A significant increase in ROS production was observed in A2780/WT cells that were treated with Doxo and US with a maximum being observed 5 min after treatment, followed by a progressive decrease over time (Fig. 4A). Interestingly, no significant ROS production was observed over time in A2780/ADR cells (Fig. 4B).

Effect *of the sonodynamic activation of doxorubicin on cell-cycle, gene expression and cell death.*

To deeply explore the effect of SDT with Doxo, a cell-cycle analysis was performed 36 h after treatment, by incubating cells with Vybrant® cell dye. A similar effect of SDT was observed in both cell lines; a block of the cell-cycle in the G_2/M phase (Fig. 5A,B). Specifically, in A2780/WT cells, a significant increase in the cell percentage of the G_2/M phase (55.80 ± 11.80 %, $p \leq 0.001$) was observed along with a significant decrease in the percentage of the G_0/G_1 phase (25.30 ± 4.80 %, $p \leq 0.01$), compared to the cell-cycle distribution of untreated cells. Likewise, in A2780/ADR cells, a strong increase in the cell percentage of the G_2/M phase (71.50 ± 17.80 %, $p \leq 0.001$) was observed along with a significant decrease in the cell percentage of the G_0/G_1 phase (10.70 ± 4.20, $p \leq 0.001$). These data led us to the conclusion that SDT with Doxo is able to induce a block in the cell-cycle in the G_2/M phase both in A2780/WT and in A2780/ADR cells.

The data obtained from cell-cycle analyses stimulated us to evaluate the mRNA expression levels of some of the genes related to the cell-cycle. Specifically, we investigated the expression of i) the *CDKN1A* gene, which codes for the cyclin-dependent kinase inhibitor p21 [46], whose effects are considered to be exerted during the G_1 phase of the cell-cycle, ii) the *CDK1* gene, which codes for a cyclin-dependent kinase 1 that is directly bound by CDKN1A kinase and that drives cells through the G_2/M phase and iii) the *TP53* gene, which codes for tumour suppressor p53. It was only possible to observe a significant modification in gene expression, compared to untreated cells, for *CDKN1A*, whose expression significantly increased after SDT with Doxo in both cell lines (15.05 ± 3.30, $p \leq 0.01$ in A2780/WT cells, Fig. 5C, and 6.07 ± 1.49, $p \leq 0.01$ in A2780/ADR cells, Fig. 5D). Moreover, a slight increase in *CDKN1A* gene expression was also noticed in A2780/WT cells when they were treated with Doxo alone, although this modification was not statistically significant. Since no difference in *TP53* gene expression was noticed in the A2780/WT and A2780/ADR cell lines, we can hypothesise the possible upregulation of CDKN1A via a p53-independent pathway in correlation with a block of the cell-cycle in the G_2/M phase.

The cell death induced in A2780/WT and A2780ADR cells by SDT with Doxo was then evaluated 36 h after treatment in a flow cytometric assay (Fig. 5E-H). In A2780/WT cells, a significant increase in early

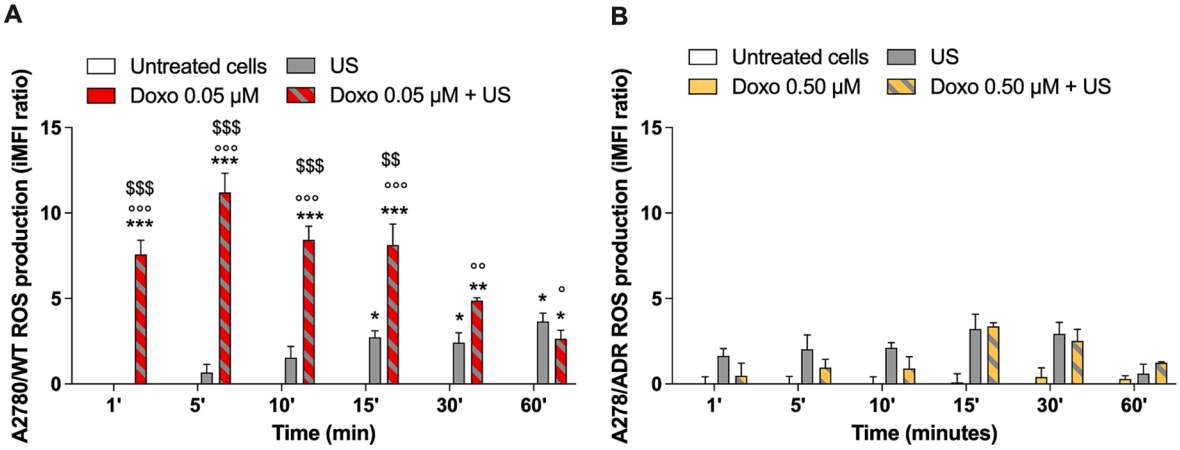

Fig. 4. Effects on ROS production of SDT with Doxo in A2780/WT and A2780/ADR cells. A2780/WT and A2780/ADR cells were incubated with 0.05 μM or 0.50 μM of Doxo for 24 or 1 h, respectively. In order to find out ROS, 2′,7′-dichlorofluorescein diacetate (DCFH-DA) was incubated with cells for 30 min and, at the end of incubation, underwent to US exposure (2.0 W/cm^2 at 1.866 MHz, 50 % DC-, for 5 min). ROS production in A2780/WT (A) and in A2780/ADR (B) cells is shown as the integrated mean fluorescence (iMFI) ratio. Statistical significance *versus* untreated cells: ** $p \leq 0.01$, *** $p \leq 0.001$, *versus* Doxo: ° $p \leq 0.05$, °° $p \leq 0.01$, °°° $p \leq 0.001$ and *versus* US: $$ $p \leq 0.01$, $$$ $p \leq 0.001$.

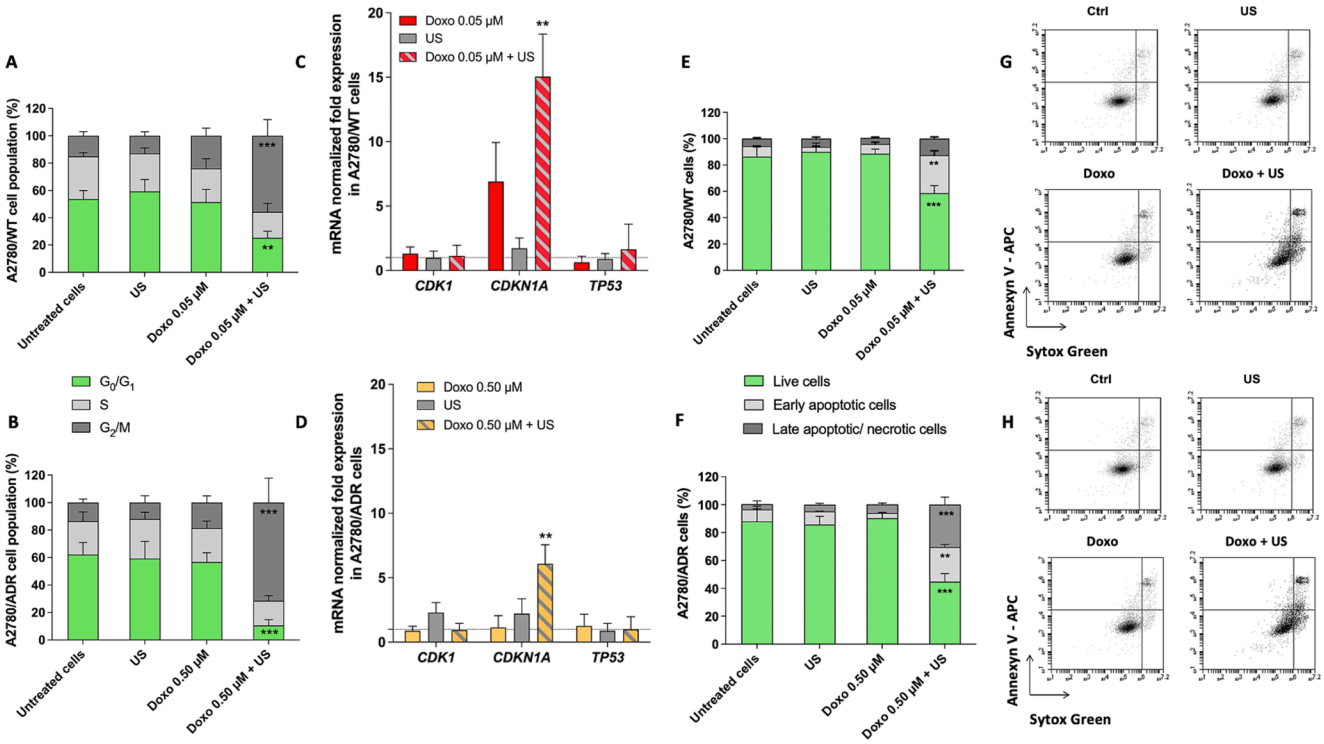

Fig. 5. Effect of SDT with Doxo on cell-cycle distribution, gene expression and cell death in A2780/WT and A2780/ADR cells. A2780/WT and A2780/ADR cells were incubated with Doxo 0.05 μM for 24 h and Doxo 0.50 μM for 1 h, respectively, and then underwent to US expsoure (2.0 W/cm^2 at 1.866 MHz, 50 % DC-, for 5 min). The cell-cycle was investigated in A2780/WT (A) and A2780/ADR (B) cells 36 h after the treatment using Vibrant® cell dye and flow cytometry. Gene expression was investigated in A2780/WT (C) and A2780/ADR (D) cells 24 h after treatment by real time RT-PCR using *RRN18S* as the reference gene (dotted lines represent untreated cells). Cell death was investigated in A2780/WT (E) and A2780/ADR (F) cells 36 h after the treatment using APC-Annexin V and Sytox® Green and flow cytometry; representative dot plots are shown (G, A2780/WT and H, A2780/ADR cells). Data are shown as mean ± standard deviation (n = 3). Statistical significance *versus* untreated cells: ** $p \leq 0.01$, *** $p \leq 0.001$. (For interpretation of the references to colour in this figure legend, the reader is referred to the web version of this article.)

apoptotic cells (28.76 ± 3.40, $p \leq 0.01$), a significant enhancement in late apoptotic/ necrotic cells (12.56 ± 1.32) and a significant reduction in live cells (58.68 ± 5.67, $p \leq 0.001$), all compared to untreated cells, were observed after SDT with Doxo, and no significant differences were observed after the other treatment conditions. Moreover, in A2780/ADR cells, a significant increase in early apoptotic cells (24.96 ± 1.78, $p \leq 0.001$), a significant increase in late apoptotic/ necrotic cells (30.50 ± 5.25, $p \leq 0.01$) and a significant reduction in live cells (44.70 ± 5.80, $p \leq 0.001$) cells, all compared to untreated cells were also detected after SDT with Doxo, and no significant differences were observed after the other treatment conditions.

3.4. *Effects of sonodynamic activation of doxorubicin on DNA damage, lipid peroxidation and mitochondrial-membrane potential*

To more thoroughly study the effects of the SDT with Doxo in A2780/WT and A2780/ADR cells, the effects on DNA damage, lipid peroxidation and mitochondrial-membrane potential have been investigated. Since Doxo is a drug that can exert its anticancer activity directly on the DNA level, an analysis of the possible DNA damage as a result of the combination of Doxo and US was investigated. Specifically, a colorimetric assay was performed, and the level of DNA damage was quantified using an aldehyde reactive probe (ARP) that specifically binds apurinic/apyrimidinic (AP) sites, which are one of the major DNA lesions [47]. Higher DNA damage was observed in A2780/WT cells ($p \leq 0.01$, Fig. 6A) than in A2780/ADR cells ($p \leq 0.05$, Fig. 6B).

Lipid peroxidation is an index of cell oxidative damage [48], as free radicals take electrons from the lipids leading to cell damage. A slight increase in lipid peroxidation was observed in A2780/WT cells ($p \leq 0.05$, Fig. 6C), while a larger increase was observed in A2780/ADR cells ($p \leq 0.01$, Fig. 6D).

Together with ROS production, reported in Fig. 4, we also monitored the treatment's influence on mitochondrial-membrane potential, as it has been reported that the ROS produced by Doxo can have a direct action on mitochondria, provoking their dysfunction and leading to a progressive decrease in mitochondrial-membrane potential [49,50]. Mitochondrial-membrane potential was evaluated after SDT with Doxo using JC-1, a fluorescent cationic carbocyanine dye, and flow cytometry. Data are showed as the ratio between JC-1 aggregates and monomers; a high proportion of monomers indicates that the depolarization of mitochondrial-membrane potential took place [51]. A significant reduction in mitochondrial-membrane potential was observed in A2780/WT cells when they underwent SDT with Doxo ($p \leq 0.01$, Fig. 6E), while only a slight reduction was detected in A2780/ADR cells ($p \leq 0.05$, Fig. 6F). At the same, time no statistically significant differences in mitochondrial-membrane potential were detected when A2780/WT and A2780/ADR cells were exposed to Doxo only.

3.5. *Doxorubicin intracellular distribution in A2780/WT and A2780/ADR cells*

A deep investigation into Doxo intracellular distribution was performed because slight differences in cell death and viability, but strong differences in ROS production, were observed in A2780/WT and A2780/ADR cells after SDT with Doxo. Briefly, A2780/WT and A2780/ADR cells were seeded on glass slides and then incubated with 0.05 μM for 24 h and 0.50 μM for 1 h, respectively. Using fluorescence microscopy, it was observed that Doxo mainly had nuclear localisation in A2780/WT cells (Fig. 7C) and spot distribution around the cell membrane in A2780/ADR cells (Fig. 7F). The different distribution patterns of Doxo in the two

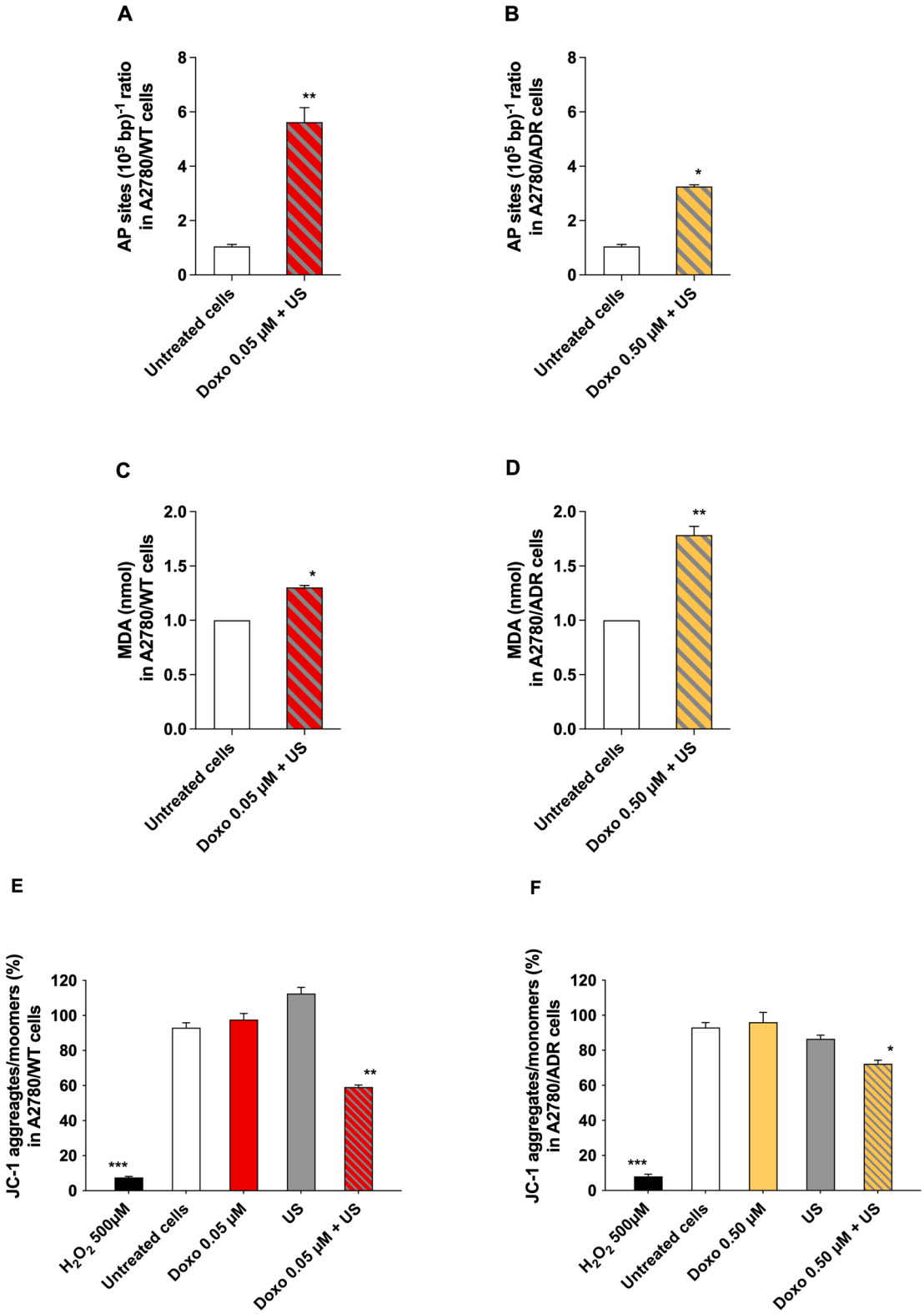

Fig. 6. Evaluation of DNA damage, lipid peroxidation and mitochondrial-membrane potential induced by SDT with Doxo in A2780/WT and A2780/ADR cells. A2780/WT (A, C and E) and A2780/ADR (B, D and F) cells were incubated with 0.05 μM and 0.50 μM Doxo for 24 h and 1 h, respectively. When the Doxo incubation ended, cells underwent to US exposure (2.0 W/cm^2 at 1.866 MHz, 50 % DC-, for 5 min). (A-B) DNA damage was detected 36 h after treatment using a fluorimetric assay and is shown as total number of AP (apurinic/apyrimidinic) sites per 10^5 bp. (C-D) Malondialdehyde (MDA) quantification, used as a lipid peroxidation index, was performed 36 h after treatment. (E-F) JC-1 assay was used to detect mitochondrial-membrane potential investigated by flow cytometry, 1 h after treatment, and is shown as the ratio between JC-1 aggregates and monomers. Data are shown as mean ± standard deviation (n = 3). Statistical significance *versus* untreated cells: * $p \leq 0.05$, ** $p \leq 0.01$, *** $p \leq 0.001$.

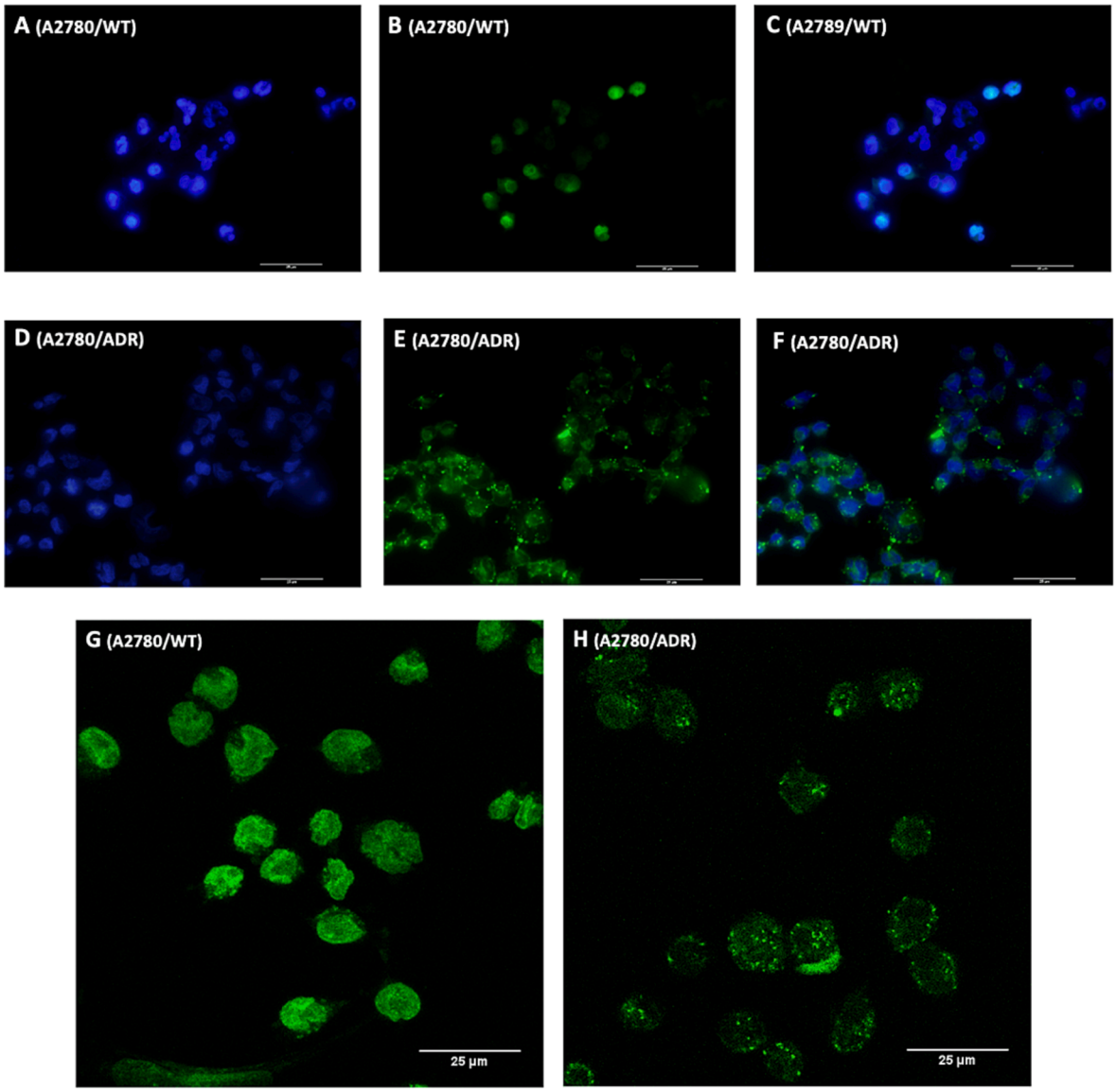

Fig. 7. Representative fluorescent and confocal imagines of doxorubicin distribution in ovarian cancer cells. A2780/WT and A2780/ADR cells were incubated with Doxo 0.05 μM for 24 h and with 0.50 μM for 1 h, respectively. A-F) fluorescent imagines showing cell nuclei stained with DAPI (blue, A and D), intracellular Doxo (green, B and E) and overlay imagines of cell nuclei and intracellular Doxo (C and F). Magnification 40x and scale bars 25 μm. G-H) confocal imagines showing Doxo distribution in ovarian cancer cell lines. Magnification 40x and scale bars 25 μm. (For interpretation of the references to colour in this figure legend, the reader is referred to the web version of this article.)

cell lines were also confirmed by confocal imaging, with Doxo showing nuclear localisation in the parental cell line (Fig. 7G) and spot distribution around the cell membrane in the resistant cell line (Fig. 7H).

3.6. Occurrence of specific damage-associated molecular patterns induced by sonodynamic activation of doxorubicin

CRT, a 46 kDa Ca^{2+}-binding protein, is typically localised in the lumen of the endoplasmic reticulum (ER), and possess several functions, including regulating nuclear transport, protein synthesis, cell invasion, proliferation and adhesion. CRT contributes to the specific recruitment of major histocompatibility complex (MHC) class I and to antigen presentation, allowing the apoptotic cancer cells to be eliminated by macrophages. Various studies have underlined that CRT is a considerable factor in the ICD and antitumor immunity [52], meaning that CRT exposure may be one of the most crucial checkpoints in inducing the immunogenicity of cell death [53]. CRT exposure on the on A2780/WT cell surface was evaluated 48 h after treatment and a strong increase in CRT exposure was detected, compared to untreated A2780/WT cells, after SDT with Doxo ($p \leq 0.001$, Fig. 8A), and a slight but significant increase was observed after treatment with Doxo alone ($p \leq 0.05$, Fig. 8A).

Exosomal HMGB1, together with CRT, is one of the specific DAMPs that are relevant for ICD. Indeed, released HMGB1 binds to TLR4 to induce dendritic-cell (DC) maturation, antigen presentation and subsequent CD8 + T cell-mediated cytotoxicity [52]. Compared to untreated A2780/WT cells, a significant increase in HMGB1 was only detected in A2780/WT cells only after the SDT with Doxo ($p \leq 0.01$, Fig. 8B).

ATP is another DAMP released from cells during ICD and it has been observed that its secretion from dying cells is critical for the effective starting of ICD pathway. Indeed, extracellular ATP promotes strong chemotactic effects by binding to purinergic receptor P2X7 (P2RX7) and purinergic receptor P2Y2 (P2RY2) on antigen-presenting cells (APCs) and their precursors, respectively. P2RX7 signalling triggers the NLR domain-containing protein 3 (NLRP3) inflammasome, which in turn provokes active IL-1β secretion, a pivotal cytokine for the extension of

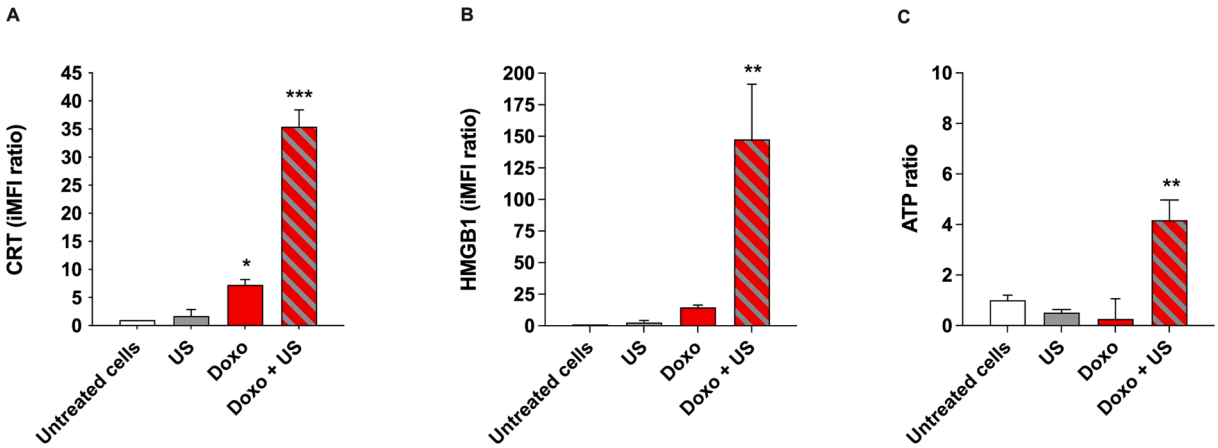

Fig. 8. Evaluation of DAMPs induced by SDT with Doxo in A2780/WT cells. A2780/WT were incubated with 0.05 μM Doxo for 24 h. When Doxo incubation ended, cells underwent to US expsoure (2.0 W/cm^2 at 1.866 MHz, 50 % DC, for 5 min). CRT (A) and HMGB1 (B) were evaluated 48 h after treatment using cytofluorimetric assays, while ATP (C) was evaluated 24 h after using a colorimetric assay. Statistical significance *versus* untreated cells: * $p \leq 0.05$, ** $p \leq 0.01$, *** $p \leq 0.001$.

antitumor immunity [52]. A significant increase in ATP was only detected in A2780/WT cells, compared to un-treated A2780/WT cells, after SDT with Doxo ($p \leq 0.01$, Fig. 8C).

4. Discussion

Ovarian cancer represents the predominant cause of death from gynaecologic malignancies and, world-wide, the second most common cancer of the female reproductive system [54,55]. Surgical debulking and platinum-based chemotherapy are the standard first-line treatment, nevertheless only 40 %–60 % of patients complete a full remission [56]. Moreover, high rates of neurotoxicity, persisting for more than a year after treatment completion, characterized this regimen [57]. For this reason, it is crucial that more efficacious and tolerable first-line alternatives are recognized. One such first-line alternatives may be Doxo in its pegylated liposomal formulation (Doxil®), in which the anthracycline is encapsulated within a sterically stabilised liposome that appears to improve the pharmacokinetics and efficacy of Doxo [58,59]. Indeed, recent clinical trials underline that combination therapy characterized by a combination of carboplatin with Doxil® may have similar or better rates of progression-free survival and similar overall survival when compared with carboplatin and paclitaxel, which is the current first-line regimen. However, these discoveries have not always been confirmed in other clinical trials [60–64]. Moreover, it has been shown that Doxo can induce drug resistance, resulting in poor patient prognosis and survival, and it is not yet known whether the use of Doxil® as a first-line treatment in the OC setting could lead to drug resistance in the second-line context, and thus negate any benefits in overall survival. In our opinion, there is a considerable need of more investigations into the use of Doxo as a first-line treatment in OC [65–67].

In this regard, Umemura and colleagues and, more recently, Fant and colleagues, have shown that US has the ability to potentiate the therapeutic effects of Doxo in the so-called SDT in murine sarcoma180 and 4T1 mammary carcinoma cell lines [32,68]. Based on the results achieved in these previous studies, our purpose was to investigate whether the same anticancer approach may be suitable for OC treatment. In order to explore this issue and overcome the main drawbacks of Doxo, such as drug resistance and its side effects, a non-cytotoxic concentration of Doxo was used and two ovarian cancer cell lines, one that is not resistant to Doxo (A2780/WT) and another that is resistant (A2780/ADR), were employed. Finally, the approach was also tested for ICD markers as patients diagnosed with OC may have recurrent cancer following initial treatment and Doxo not only triggers tumour cell death, but also evokes effective antitumor immunity responses by inducing ICD [37].

First of all, we confirmed that there is a large difference in Doxo IC_{50} values in A2780/WT and A2780/ADR cells, with a strong cytotoxic effect already being observed in A2780/WT cells at 24 h at low concentrations, while only slight cytotoxicity was observed in A2780/ADR cells at the highest concentration investigated (Fig. 2A,B). A very different cellular uptake of Doxo in A2780/WT and A2780/ADR cells was highlighted by cytofluorimetric analysis (Fig. 2C,D). These data were consistent with studies showing that the overexpression of P-gp is responsible for the high efflux of Doxo from cancer cells [69] and were confirmed by investigating P-gp activity in both cell lines using the calcein-AM assay, as calcein-AM is a well-known P-gp substrate (Fig. 2E). The maximum level of Doxo internalization over time, *i.e.* 0.05 μM for 24 h in A2780/WT cells and 0.50 μM for 1 h in A2780/ADR cells (Fig. 2), were then selected as the most suitable conditions to perform SDT experiments.

Interestingly, sonodynamic treatment was able to significantly inhibit cell proliferation in both cell lines up to 72 h, whereas Doxo and US alone did not affect cancer-cell proliferation. To the best of our knowledge, this demonstrates, for the first time, the potential synergistic effect of US and Doxo on resistant and non-resistant ovarian cancer cells (Fig. 3). Moreover, in order to avoid any misinterpretation of our results due to sonoporation having a possible role in our SDT experiments, mainly in A2780/ADR cells, a cytofluorimetric assay was performed on both cell lines (data not showed). The results show that no sonoporation phenomena occurred during SDT, leading to the assumption that US-mediated Doxo cytotoxicity is not due to an increased uptake of the drug in our set-up. This achievement was also consistent with work by Fant and colleagues in which the morphological observation of cells using confocal microscopy observations did not show any membrane poration differences in US-exposed and non-US-exposed cells [32].

Since the idea behind SDT draws inspiration from PDT, it is well accepted that the predominant mechanism of action that triggers the cytotoxic effects proceeds via the production of ROS. Therefore, in our study, we investigated whether the combination of a non-cytotoxic concentration of Doxo and US may be able to produce an increase in ROS production in OC cell lines. Significant intracellular ROS levels were observed, thanks to the DCFH-DA assay, in A2780/WT cells under SDT, as well as a lack of ROS production and very low ROS production levels after treatment with US and Doxo alone, respectively (Fig. 4A). Surprisingly, no significant ROS production was observed in A2780/ADR cells after the sonodynamic activation of Doxo (Fig. 4B). This difference in ROS production behaviour in the two cell lines may suggest that two different SDT mechanisms of action take place; ROS-dependent and ROS-independent mechanisms, as indicated by Umemmura *et al.*

and Choi and *et al.* [33,70].

Given that our experimental set-up killed A2780/WT and A2780/ADR cells in different ways, we decided to thoroughly investigate the cytotoxicity of SDT with Doxo at 36 h after the treatment by studying the cell-cycle distribution. A block in the cell cycle occurred in the G_2/M phase in both cell lines (Fig. 5A,B). We then investigated the mRNA expression of i) the cyclin dependent kinase 1 (*CDK1*) gene, whose encoded protein is critical for G_1/S and G_2/M phase transitions in eukaryotic cells, ii) the *CDKN1A* gene, whose encoded protein, termed p21, is a potent inhibitor of cyclin-dependent kinases such as the CDK1, which is essential for the regulation of cell-cycle progression, and iii) the TP53 gene, whose encoded protein, termed p53, responds to several cellular stresses to regulate the expression of target genes, such as *CDKN1A*, thereby inducing cell-cycle arrest, senescence, apoptosis, DNA repair and changes in metabolism [71,72]. Our results show that there was no difference in *CDK1* mRNA expression in the cell lines as is the case for the mRNA expression of *TP53*. However, *CDKN1A* mRNA was over-expressed in both cell lines after SDT (Fig. 5C,D). Consequently, these results suggest that SDT effectively led to G_2/M arrest in the A2780/WT and A2780/ADR cell lines via a p53-independent pathway. As it is known that ROS can lead to p53-independent G_2/M arrest in cancer cells and that the main ROS-dependent effect of Doxo on cell-cycle progression is to determine the G_2/M phase cell cycle block, we propose that SDT in the cell lines was mainly able to trigger Doxo cytotoxicity due to ROS-dependent DNA damage, although ROS production appeared not to be involved in the SDT cytotoxicity of A2780/ADR cells [73–75].

Moreover, a significant reduction in live cells was observed along with an increase in apoptotic cells in both cell lines, but, interestingly, we also observed an increase in late apoptotic/ necrotic cells in the A2780/ADR cell line, and this was not detected in A2780/WT cells, compared to untreated cells (Fig. 5E-H). Therefore, a DNA-damage analysis was carried out via the quantification of apurinic and apyrimidinic (AP) sites, which represent the main oxidative stress-mediated DNA base damage. Our data showed that both A2780/WT and A2780/ADR cells demonstrated a statistically significant increase in AP sites after SDT, compared to untreated cells, thus confirming that ROS production played a role in DNA damage. However, interestingly, a higher number of AP sites were detected in A2780/WT cells than in A2780/ADR cells (Fig. 6A,D). In order to continue our investigation into the role of oxidative stress after SDT in our cell lines, lipid peroxidation analysis was performed and the most commonly used lipid marker of oxidative stress, namely malondialdehyde (MDA), was evaluated [76]. Our results showed a significant increase in MDA content in both cell lines, compared to untreated cells, although it was much higher, this time, in A2780/ADR cells than in A2780/ADR cells (Fig. 6C,D). To complete our study of the role of the oxidative stress in OC cell lines after SDT with Doxo, an investigation of mitochondrial-membrane potential was performed because it has been reported that ROS can act directly on mitochondria, provoking their dysfunction and leading to a progressive decrease in mitochondrial-membrane potential [49,50]. Indeed, significant effect on mitochondrial-membrane depolarization was observed, compared to untreated cells, in both cell lines after SDT, although it was, again, higher in A2780/WT cells than in A2780/ADR cells (Fig. 6E,F).

Thus, taken together, these findings confirm that a ROS-dependent mechanism is the main underlying mechanism of action of SDT, and that this mechanism is responsible for killing both Doxo non-resistant and resistant cells. Although slight differences were reported, our findings, in our opinion, may explain why no ROS production was observed in A2780/ADR cells after SDT with Doxo. Indeed, more DNA damage and mitochondrial dysfunction, and less lipid peroxidation were observed in A2780/WT cells, whereas less DNA damage and mitochondrial dysfunction, and more lipid peroxidation were detected in A2780/ADR cells, suggesting that not just the intracellular level, but also the intracellular distribution of Doxo were different in the two OC cell lines. Indeed, the distribution of a sonosensitiser inside a cell is a key point when performing SDT as different SDT mechanisms of action may take place in accordance with the cellular localisation of the sonosensitiser [33,77].

Although we believe that the same SDT mechanism of action is involved in killing both OC cell lines in our work, we are aware that the different Doxo distribution in our cells may explain why no ROS production was reported in A2780/ADR cells. For this reason, we performed two microscopy investigations; the first based on fluorescence microscopy and the second based on confocal microscopy. As observed in the fluorescent and confocal imagines (Fig. 7), in A2780/WT cells, Doxo 0.05 μM was mainly localised at the nuclear level 24 h after Doxo incubation, while, in A2780/ADR, Doxo 0.50 μM was already localised at the membrane level in compact clusters 1 h after Doxo incubation. Differences in the cellular distribution of Doxo is based, of course, on differences in P-gp activity. This is also supported by the work of Burrow and colleagues in which a different Doxo localisation pattern was reported in Doxo resistant and non-resistant murine breast cancer cell lines [78]. According to the different localisation of Doxo in the A2780/WT and A2780/ADR cells and the hypothesis suggested by Krasovitski et al. [37], it may be possible to state that ROS generation after SDT targeted, mostly, DNA and mitochondria in A2780/WT cells, where Doxo was mainly localised at the nuclear level, whereas in the A2780/ADR cells, where Doxo was mainly localised close to the cell membrane, ROS generation after SDT predominantly targeted the plasma membrane [37]. This suggestion could be also confirmed by results from cell-death analyses that show that not only apoptosis occurred in A2780/ADR cells, but also necrosis due, in our opinion, to the close vicinity of the ROS generation to polyunsaturated fatty acids (PUFAs), which are mainly localised in the cell membrane [79]. This close vicinity between Doxo and the plasma membrane may also explain why we did not detect ROS generation after SDT. Indeed, the DCFH-DA assay seems to not work properly when ROS production is very close to the target (*e.g.*, phospholipids) due to the competition between, in our case, PUFAs and DCFH [80,81].

Finally, since OC with complete clinical response recurs with a high rate, a first-line therapeutic strategy that could decrease this rate would be very promising. Doxo is an anthracycline and is well known as an inducer of ICD with the possibility of increasing the antitumor immunity [82]. The proper mechanisms that characterize ICD induction is, nowadays, still not completely comprehended. However, it has been hypothesized that oxidative stress could play a crucial role. For instance, it has been suggested that some DAMPs linked with oxidative stress, like peroxidized phospholipids, can be identified by the immune system as immunogenic [83]. For this reason, the sonodynamic anticancer approach was also tested in A2780/WT cells to investigate its ability to act as an ICD inducer, with CRT cellular exposure, HMGB1 nuclear release and ATP being verified. As a matter of fact, Fig. 8 shows a significant increase in CRT cellular exposure, HMGB1 nuclear release and ATP after SDT, suggesting that the activation of Doxo through US was able to kill A2780/WT cells in a way that might activate the ICD pathway.

5. Conclusions

Chemotherapy resistance and recurrence are the most challenging issues in OC, meaning that this type of cancer remains one of the most lethal gynaecologic cancers worldwide. In this work, we have investigated a new therapeutic strategy that is based on US and Doxo, in what is called sonodynamic therapy, and we have established, for the first time, to the best of our knowledge, the effectiveness of this innovative anticancer approach in both Doxo non-resistant and resistant OC cell lines. This approach is characterised by the use of Doxo at concentrations that are harmless *per sé* but cytotoxic under US exposure and by US-mediated anticancer immune sensitisation.

Declaration of Competing Interest

The authors declare that they have no known competing financial interests or personal relationships that could have appeared to influence the work reported in this paper.

Data availability

Data will be made available on request.

Acknowledgments

This research was funded by Associazione Italiana per la Ricerca sul Cancro (AIRC, IG-22041) and the University of Torino (Ricerca Locale 2021). The authors would like to thank Dale James Matthew Lawson for his critical proofreading and advice.

References

[1] B.T. Hennessy, R.L. Coleman, M. Markman, Ovarian cancer, The Lancet. 374 (2009) 1371–1382, https://doi.org/10.1016/S0140-6736(09)61338-6.
[2] F.A. Raja, N. Chopra, J.A. Ledermann, Optimal first-line treatment in ovarian cancer, Annals of Oncology. 23 (2012) x118–x127, https://doi.org/10.1093/annonc/mds315.
[3] R. Brett M., P. Jennifer B., S. Thomas A., R. Brett M., P. Jennifer B., S. Thomas A., Epidemiology of ovarian cancer: a review, Cancer Biol Med. 14 (2017) 9–32. https://doi.org/10.20892/j.issn.2095-3941.2016.0084.
[4] A. Gadducci, V. Guarneri, F.A. Peccatori, G. Ronzino, G. Scandurra, C. Zamagni, P. Zola, V. Salutari, Current strategies for the targeted treatment of high-grade serous epithelial ovarian cancer and relevance of BRCA mutational status, J Ovarian Res. 12 (2019) 9, https://doi.org/10.1186/s13048-019-0484-6.
[5] S. Boussios, P. Karihtala, M. Moschetta, A. Karathanasi, A. Sadauskaite, E. Rassy, N. Pavlidis, Combined Strategies with Poly (ADP-Ribose) Polymerase (PARP) Inhibitors for the Treatment of Ovarian Cancer: A Literature Review, Diagnostics. 9 (2019) 87, https://doi.org/10.3390/diagnostics9030087.
[6] P. Vikas, N. Borcherding, A. Chennamadhavuni, R. Garje, Therapeutic Potential of Combining PARP Inhibitor and Immunotherapy in Solid Tumors, Front Oncol. 10 (2020), https://doi.org/10.3389/fonc.2020.00570.
[7] S. Sundar, R.D. Neal, S. Kehoe, Diagnosis of ovarian cancer, BMJ. (2015) h4443. https://doi.org/10.1136/bmj.h4443.
[8] A. Chandra, C. Pius, M. Nabeel, M. Nair, J.K. Vishwanatha, S. Ahmad, R. Basha, Ovarian cancer: Current status and strategies for improving therapeutic outcomes, Cancer Med. 8 (2019) 7018–7031, https://doi.org/10.1002/cam4.2560.
[9] J. Fanning, T.Z. Bennett, R.D. Hilgers, Meta-analysis of cisplatin, doxorubicin, and cyclophosphamide versus cisplatin and cyclophosphamide chemotherapy of ovarian carcinoma, Obstetrics and Gynecology. 80 (1992) 954–960.
[10] C.F. Thorn, C. Oshiro, S. Marsh, T. Hernandez-Boussard, H. McLeod, T.E. Klein, R. B. Altman, Doxorubicin pathways, Pharmacogenet Genomics. 21 (2011) 440–446, https://doi.org/10.1097/FPC.0b013e32833ffb56.
[11] K.C. Nitiss, J.L. Nitiss, Twisting and Ironing: Doxorubicin Cardiotoxicity by Mitochondrial DNA Damage, Clinical Cancer Research. 20 (2014) 4737–4739, https://doi.org/10.1158/1078-0432.CCR-14-0821.
[12] G. Shim, S. Manandhar, D. Shin, T.-H. Kim, M.-K. Kwak, Acquisition of doxorubicin resistance in ovarian carcinoma cells accompanies activation of the NRF2 pathway, Free Radic Biol Med. 47 (2009) 1619–1631, https://doi.org/10.1016/j.freeradbiomed.2009.09.006.
[13] M.M. Gottesman, Mechanisms of Cancer Drug Resistance, Annu Rev Med. 53 (2002) 615–627, https://doi.org/10.1146/annurev.med.53.082901.103929.
[14] M.M. Gottesman, V. Ling, The molecular basis of multidrug resistance in cancer: The early years of P-glycoprotein research, FEBS Lett. 580 (2006) 998–1009, https://doi.org/10.1016/j.febslet.2005.12.060.
[15] C. Pisano, S.C. Cecere, M. di Napoli, C. Cavaliere, R. Tambaro, G. Facchini, C. Scaffa, S. Losito, A. Pizzolorusso, S. Pignata, Clinical Trials with Pegylated Liposomal Doxorubicin in the Treatment of Ovarian Cancer, J Drug Deliv. 2013 (2013) 1–12, https://doi.org/10.1155/2013/898146.
[16] A.A. Gabizon, Pegylated Liposomal Doxorubicin: Metamorphosis of an Old Drug into a New Form of Chemotherapy, Cancer Invest. 19 (2001) 424–436, https://doi.org/10.1081/CNV-100103136.
[17] M. Markman, M.A. Bookman, Second-Line Treatment of Ovarian Cancer, Oncologist. 5 (2000) 26–35, https://doi.org/10.1634/theoncologist.5-1-26.
[18] T.A. Lawrie, R. Rabbie, C. Thoma, J. Morrison, Pegylated liposomal doxorubicin for first-line treatment of epithelial ovarian cancer, in: T.A. Lawrie (Ed.), Cochrane Database of Systematic Reviews, John Wiley & Sons Ltd, Chichester, UK, 2013, https://doi.org/10.1002/14651858.CD010482.
[19] A.E. Green, P.G. Rose, Pegylated liposomal doxorubicin in ovarian cancer, Int J Nanomedicine. 1 (2006) 229–239.
[20] F. Wilkinson, W.P. Helman, A.B. Ross, Quantum Yields for the Photosensitized Formation of the Lowest Electronically Excited Singlet State of Molecular Oxygen in Solution, J Phys Chem Ref Data. 22 (1993) 113–262, https://doi.org/10.1063/1.555934.
[21] R.W. Redmond, J.N. Gamlin, A Compilation of Singlet Oxygen Yields from Biologically Relevant Molecules, Photochem Photobiol. 70 (1999) 391–475, https://doi.org/10.1111/j.1751-1097.1999.tb08240.x.
[22] R. Ruiz-González, P. Milán, R. Bresolí-Obach, J. Stockert, A. Villanueva, M. Cañete, S. Nonell, Photodynamic Synergistic Effect of Pheophorbide a and Doxorubicin in Combined Treatment against Tumoral Cells, Cancers (Basel). 9 (2017) 18, https://doi.org/10.3390/cancers9020018.
[23] J.C. Cacaccio, F.A. Durrani, J.R. Missert, R.K. Pandey, Photodynamic Therapy in Combination with Doxorubicin Is Superior to Monotherapy for the Treatment of Lung Cancer, Biomedicines. 10 (2022) 857, https://doi.org/10.3390/biomedicines10040857.
[24] G. Streckyte, J. Didziapetriene, G. Grazeliene, G. Prasmickiene, D. Sukeliene, N. Kazlauskaite, D. Characiejus, L. Griciute, R. Rotomskis, Effects of photodynamic therapy in combination with Adriamycin, Cancer Lett. 146 (1999) 73–86, https://doi.org/10.1016/S0304-3835(99)00241-4.
[25] K. Logan, F. Foglietta, H. Nesbitt, Y. Sheng, T. McKaig, S. Kamila, J. Gao, N. Nomikou, B. Callan, A.P. McHale, J.F. Callan, Targeted chemo-sonodynamic therapy treatment of breast tumours using ultrasound responsive microbubbles loaded with paclitaxel, doxorubicin and Rose Bengal, European Journal of Pharmaceutics and Biopharmaceutics. 139 (2019) 224–231, https://doi.org/10.1016/j.ejpb.2019.04.003.
[26] T. Li, Y.-N. Wang, T.D. Khokhlova, S. D'Andrea, F. Starr, H. Chen, J.S. McCune, L. J. Risler, A. Mashadi-Hossein, S.R. Hingorani, A. Chang, J.H. Hwang, Pulsed High-Intensity Focused Ultrasound Enhances Delivery of Doxorubicin in a Preclinical Model of Pancreatic Cancer, Cancer Res. 75 (2015) 3738–3746, https://doi.org/10.1158/0008-5472.CAN-15-0296.
[27] J. Piron, K. Kaddur, A. Bouakaz, K. Hynynen, J. Souquet, Enhancement of doxorubicin effect on cancer cell mortality with ultrasound and microbubbles, in (2010) 161–163, https://doi.org/10.1063/1.3367131.
[28] T. Yoshida, T. Kondo, R. Ogawa, L.B. Feril, Q.-L. Zhao, A. Watanabe, K. Tsukada, Combination of doxorubicin and low-intensity ultrasound causes a synergistic enhancement in cell killing and an additive enhancement in apoptosis induction in human lymphoma U937 cells, Cancer Chemother Pharmacol. 61 (2008) 559–567, https://doi.org/10.1007/s00280-007-0503-y.
[29] B. Helfield, X. Chen, S.C. Watkins, F.S. Villanueva, Biophysical insight into mechanisms of sonoporation, Proceedings of the National Academy of Sciences. 113 (2016) 9983–9988. https://doi.org/10.1073/pnas.1606915113.
[30] J. Qin, T.-Y. Wang, J.K. Willmann, Sonoporation: Applications for Cancer Therapy, in: 2016: pp. 263–291. https://doi.org/10.1007/978-3-319-22536-4_15.
[31] A. Bouakaz, A. Zeghimi, A.A. Doinikov, Sonoporation: Concept and Mechanisms, in: 2016: pp. 175–189. https://doi.org/10.1007/978-3-319-22536-4_10.
[32] C. Fant, M. Lafond, B. Rogez, I.S. Castellanos, J. Ngo, J.-L. Mestas, F. Padilla, C. Lafon, In vitro potentiation of doxorubicin by unseeded controlled non-inertial ultrasound cavitation, Sci Rep. 9 (2019) 15581, https://doi.org/10.1038/s41598-019-51785-7.
[33] V. Choi, M.A. Rajora, G. Zheng, Activating Drugs with Sound: Mechanisms Behind Sonodynamic Therapy and the Role of Nanomedicine, Bioconjug Chem. 31 (2020) 967–989, https://doi.org/10.1021/acs.bioconjchem.0c00029.
[34] M. Lafond, S. Yoshizawa, S. Umemura, Sonodynamic Therapy: Advances and Challenges in Clinical Translation, Journal of Ultrasound in Medicine. 38 (2019) 567–580, https://doi.org/10.1002/jum.14733.
[35] F. Giuntini, F. Foglietta, A.M. Marucco, A. Troia, N. v. Dezhkunov, A. Pozzoli, G. Durando, I. Fenoglio, L. Serpe, R. Canaparo, Insight into ultrasound-mediated reactive oxygen species generation by various metal-porphyrin complexes, Free Radic Biol Med. 121 (2018) 190–201. https://doi.org/10.1016/j.freeradbiomed.2018.05.002.
[36] R. Canaparo, F. Foglietta, F. Giuntini, A. Francovich, L. Serpe, The bright side of sound: perspectives on the biomedical application of sonoluminescence, Photochemical & Photobiological Sciences. 19 (2020) 1114–1121, https://doi.org/10.1039/D0PP00133C.
[37] B. Krasovitski, V. Frenkel, S. Shoham, E. Kimmel, Intramembrane cavitation as a unifying mechanism for ultrasound-induced bioeffects, Proceedings of the National Academy of Sciences. 108 (2011) 3258–3263. https://doi.org/10.1073/pnas.1015771108.
[38] Y. Liu, H. Bai, K. Guo, P. Wang, Hypocrellin B triggered sonodynamic therapy reverses multidrug resistance of doxorubicin-resistant SGC7901/ADR cells via down-regulation of P-gp expression, Journal of Chemotherapy. 32 (2020) 385–393, https://doi.org/10.1080/1120009X.2020.1778242.
[39] N. Casares, M.O. Pequignot, A. Tesniere, F. Ghiringhelli, S. Roux, N. Chaput, E. Schmitt, A. Hamai, S. Hervas-Stubbs, M. Obeid, F. Coutant, D. Métivier, E. Pichard, P. Aucouturier, G. Pierron, C. Garrido, L. Zitvogel, G. Kroemer, Caspase-dependent immunogenicity of doxorubicin-induced tumor cell death, Journal of Experimental Medicine. 202 (2005) 1691–1701, https://doi.org/10.1084/jem.20050915.
[40] Q. Zhang, C. Bao, X. Cai, L. Jin, L. Sun, Y. Lang, L. Li, Sonodynamic therapy-assisted immunotherapy: A novel modality for cancer treatment, Cancer Sci. 109 (2018) 1330–1345, https://doi.org/10.1111/cas.13578.
[41] T. Bruns, J. Peter, S. Hagel, A. Herrmann, A. Stallmach, The augmented neutrophil respiratory burst in response to *Escherichia coli* is reduced in liver cirrhosis during infection, Clin Exp Immunol. 164 (2011) 346–356, https://doi.org/10.1111/j.1365-2249.2011.04373.x.
[42] Y.-T. Chang, C.C.N. Wang, J.-Y. Wang, T.-E. Lee, Y.-Y. Cheng, S.L. Morris-Natschke, K.-H. Lee, C.-C. Hung, Tenulin and isotenulin inhibit P-glycoprotein function and overcome multidrug resistance in cancer cells, Phytomedicine. 53 (2019) 252–262, https://doi.org/10.1016/j.phymed.2018.09.008.

[43] S.A. Bustin, V. Benes, J.A. Garson, J. Hellemans, J. Huggett, M. Kubista, R. Mueller, T. Nolan, M.W. Pfaffl, G.L. Shipley, J. Vandesompele, C.T. Wittwer, The MIQE Guidelines: Minimum Information for Publication of Quantitative Real-Time PCR Experiments, Clin Chem. 55 (2009) 611–622, https://doi.org/10.1373/clinchem.2008.112797.
[44] E. Matuszewska, D. Leszczyńska, D. Kuczyńska-Wiśnik, M.M. Algara, K. Stojowska, M. Augustynowicz, E. Laskowska, Lack of intracellular trehalose affects formation of Escherichia coli persister cells, Microbiology (N Y). 161 (2015) 786–796, https://doi.org/10.1099/mic.0.000012.
[45] D. Cappetta, A. de Angelis, L. Sapio, L. Prezioso, M. Illiano, F. Quaini, F. Rossi, L. Berrino, S. Naviglio, K. Urbanek, Oxidative Stress and Cellular Response to Doxorubicin: A Common Factor in the Complex Milieu of Anthracycline Cardiotoxicity, Oxid Med Cell Longev. 2017 (2017) 1–13, https://doi.org/10.1155/2017/1521020.
[46] K. Engeland, Cell cycle regulation: p53–p21-RB signaling, Cell Death Differ. 29 (2022) 946–960, https://doi.org/10.1038/s41418-022-00988-z.
[47] S. Kurisu, T. Miya, H. Terato, A. Masaoka, Y. Ohyama, K. Kubo, H. Ide, Quantitation of DNA damage by an aldehyde reactive probe (ARP), Nucleic Acids Symp Ser. 1 (2001) 45–46, https://doi.org/10.1093/nass/1.1.45.
[48] Q. Tan, X. Yan, L. Song, H. Yi, P. Li, G. Sun, D. Yu, L. Li, Z. Zeng, Z. Guo, Induction of Mitochondrial Dysfunction and Oxidative Damage by Antibiotic Drug Doxycycline Enhances the Responsiveness of Glioblastoma to Chemotherapy, Medical Science Monitor. 23 (2017) 4117–4125, https://doi.org/10.12659/MSM.903245.
[49] S. Gorini, A. de Angelis, L. Berrino, N. Malara, G. Rosano, E. Ferraro, Chemotherapeutic Drugs and Mitochondrial Dysfunction: Focus on Doxorubicin, Trastuzumab, and Sunitinib, Oxid Med Cell Longev. 2018 (2018) 1–15, https://doi.org/10.1155/2018/7582730.
[50] F. Sivandzade, A. Bhalerao, L. Cucullo, Analysis of the Mitochondrial Membrane Potential Using the Cationic JC-1 Dye as a Sensitive Fluorescent Probe, Bio Protoc. 9 (2019), https://doi.org/10.21769/BioProtoc.3128.
[51] E. Synowiec, G. Hoser, J. Bialkowska-Warzecha, E. Pawlowska, T. Skorski, J. Blasiak, Doxorubicin Differentially Induces Apoptosis, Expression of Mitochondrial Apoptosis-Related Genes, and Mitochondrial Potential in BCR-ABL1-Expressing Cells Sensitive and Resistant to Imatinib, Biomed Res Int. 2015 (2015) 1–9, https://doi.org/10.1155/2015/673512.
[52] Z. Asadzadeh, E. Safarzadeh, S. Safaei, A. Baradaran, A. Mohammadi, K. Hajiasgharzadeh, A. Derakhshani, A. Argentiero, N. Silvestris, B. Baradaran, Current Approaches for Combination Therapy of Cancer: The Role of Immunogenic Cell Death, Cancers (Basel). 12 (2020) 1047, https://doi.org/10.3390/cancers12041047.
[53] G. Kroemer, L. Galluzzi, O. Kepp, L. Zitvogel, Immunogenic Cell Death in Cancer Therapy, Annu Rev Immunol. 31 (2013) 51–72, https://doi.org/10.1146/annurev-immunol-032712-100008.
[54] G. Tortolero-Luna, M.F. Mitchell, The epidemiology of ovarian cancer, J Cell Biochem. 59 (1995) 200–207, https://doi.org/10.1002/jcb.240590927.
[55] M. Piechocki, W. Koziołek, D. Sroka, A. Matrejek, P. Miziołek, N. Saiuk, M. Sledzik, A. Jaworska, K. Bereza, E. Pluta, T. Banas, Trends in Incidence and Mortality of Gynecological and Breast Cancers in Poland (1980–2018), Clin Epidemiol. 14 (2022) 95–114, https://doi.org/10.2147/CLEP.S330081.
[56] A. Kim, Y. Ueda, T. Naka, T. Enomoto, Therapeutic strategies in epithelial ovarian cancer, Journal of Experimental & Clinical Cancer Research. 31 (2012) 14, https://doi.org/10.1186/1756-9966-31-14.
[57] S. Pignata, S. de Placido, R. Biamonte, G. Scambia, G. di Vagno, G. Colucci, A. Febbraro, M. Marinaccio, A. Vernaglia Lombardi, L. Manzione, G. Cartenì, M. Nardi, S. Danese, M.R. Valerio, A. de Matteis, B. Massidda, G. Gasparini, M. di Maio, C. Pisano, F. Perrone, Residual neurotoxicity in ovarian cancer patients in clinical remission after first-line chemotherapy with carboplatin and paclitaxel: The Multicenter Italian Trial in Ovarian cancer (MITO-4) retrospective study, BMC Cancer. 6 (2006) 5. https://doi.org/10.1186/1471-2407-6-5.
[58] D.C. Drummond, O. Meyer, K. Hong, D.B. Kirpotin, D. Papahadjopoulos, Optimizing liposomes for delivery of chemotherapeutic agents to solid tumors, Pharmacol Rev. 51 (1999) 691–743.
[59] T. Thigpen, A Rational Approach to the Management of Recurrent or Persistent Ovarian Carcinoma, Clin Obstet Gynecol. 55 (2012) 114–130, https://doi.org/10.1097/GRF.0b013e31824b9bc5.
[60] J.A. Rakowski, S. Ahmad, R.W. Holloway, Use of pegylated liposomal doxorubicin in the management of platinum-sensitive recurrent ovarian cancer: current concepts, Expert Rev Anticancer Ther. 12 (2012) 31–40, https://doi.org/10.1586/era.11.187.
[61] U. Wagner, C. Marth, R. Largillier, J. Kaern, C. Brown, M. Heywood, T. Bonaventura, I. Vergote, M.C. Piccirillo, R. Fossati, V. Gebski, E.P. Lauraine, Final overall survival results of phase III GCIG CALYPSO trial of pegylated liposomal doxorubicin and carboplatin vs paclitaxel and carboplatin in platinum-sensitive ovarian cancer patients, Br J Cancer. 107 (2012) 588–591, https://doi.org/10.1038/bjc.2012.307.
[62] S. Pignata, G. Scambia, G. Ferrandina, A. Savarese, R. Sorio, E. Breda, V. Gebbia, P. Musso, L. Frigerio, P. del Medico, A.V. Lombardi, A. Febbraro, P. Scollo, A. Ferro, S. Tamberi, A. Brandes, A. Ravaioli, M.R. Valerio, E. Aitini, D. Natale, L. Scaltriti, S. Greggi, C. Pisano, D. Lorusso, V. Salutari, F. Legge, M. di Maio, A. Morabito, C. Gallo, F. Perrone, Carboplatin Plus Paclitaxel Versus Carboplatin Plus Pegylated Liposomal Doxorubicin As First-Line Treatment for Patients With Ovarian Cancer: The MITO-2 Randomized Phase III Trial, Journal of Clinical Oncology. 29 (2011) 3628–3635, https://doi.org/10.1200/JCO.2010.33.8566.
[63] D. Bafaloukos, H. Linardou, G. Aravantinos, C. Papadimitriou, A. Bamias, G. Fountzilas, H.P. Kalofonos, P. Kosmidis, E. Timotheadou, T. Makatsoris, E. Samantas, E. Briasoulis, C. Christodoulou, P. Papakostas, D. Pectasides, A. M. Dimopoulos, A randomized phase II study of carboplatin plus pegylated liposomal doxorubicin versus carboplatin plus paclitaxel in platinum sensitive ovarian cancer patients: a Hellenic Cooperative Oncology Group study, BMC Med. 8 (2010) 3, https://doi.org/10.1186/1741-7015-8-3.
[64] M. Brundage, M. Gropp, F. Mefti, K. Mann, B. Lund, V. Gebski, G. Wolfram, N. Reed, S. Pignata, A. Ferrero, C. Brown, E. Eisenhauer, E. Pujade-Lauraine, Health-related quality of life in recurrent platinum-sensitive ovarian cancer—results from the CALYPSO trial, Annals of Oncology. 23 (2012) 2020–2027, https://doi.org/10.1093/annonc/mdr583.
[65] J. Cox, S. Weinman, Mechanisms of doxorubicin resistance in hepatocellular carcinoma, Hepat, Oncol. 3 (2016) 57–59, https://doi.org/10.2217/hep.15.41.
[66] C. Christowitz, T. Davis, A. Isaacs, G. van Niekerk, S. Hattingh, A.-M. Engelbrecht, Mechanisms of doxorubicin-induced drug resistance and drug resistant tumour growth in a murine breast tumour model, BMC Cancer. 19 (2019) 757, https://doi.org/10.1186/s12885-019-5939-z.
[67] J.-M. Gibson, S. Alzghari, C. Ahn, H. Trantham, N.M. La-Beck, The Role of Pegylated Liposomal Doxorubicin in Ovarian Cancer: A Meta-Analysis of Randomized Clinical Trials, Oncologist. 18 (2013) 1022–1031, https://doi.org/10.1634/theoncologist.2013-0126.
[68] S. Umemura, N. Yumita, Y. Okano, M. Kaneuchi, N. Magario, M. Ishizaki, K. Shimizu, Y. Sano, K. Umemura, R. Nishigaki, Sonodynamically-induced in vitro cell damage enhanced by adriamycin, Cancer Lett. 121 (1997) 195–201, https://doi.org/10.1016/S0304-3835(97)00354-6.
[69] S. Mirzaei, M.H. Gholami, F. Hashemi, A. Zabolian, M.V. Farahani, K. Hushmandi, A. Zarrabi, A. Goldman, M. Ashrafizadeh, G. Orive, Advances in understanding the role of P-gp in doxorubicin resistance: Molecular pathways, therapeutic strategies, and prospects, Drug Discov Today. 27 (2022) 436–455, https://doi.org/10.1016/j.drudis.2021.09.020.
[70] L.B. Feril, T. Kondo, Z.-G. Cui, Y. Tabuchi, Q.-L. Zhao, H. Ando, T. Misaki, H. Yoshikawa, S. Umemura, Apoptosis induced by the sonomechanical effects of low intensity pulsed ultrasound in a human leukemia cell line, Cancer Lett. 221 (2005) 145–152, https://doi.org/10.1016/j.canlet.2004.08.034.
[71] K.J. Barnum, M.J. O'Connell, Cell Cycle Regulation by Checkpoints, in: 2014: pp. 29–40. https://doi.org/10.1007/978-1-4939-0888-2_2.
[72] N. Hustedt, D. Durocher, The control of DNA repair by the cell cycle, Nat Cell Biol. 19 (2017) 1–9, https://doi.org/10.1038/ncb3452.
[73] S. Macip, A. Kosoy, S.W. Lee, M.J. O'Connell, S.A. Aaronson, Oxidative stress induces a prolonged but reversible arrest in p53-null cancer cells, involving a Chk1-dependent G2 checkpoint, Oncogene. 25 (2006) 6037–6047, https://doi.org/10.1038/sj.onc.1209629.
[74] U.S. Srinivas, B.W.Q. Tan, B.A. Vellayappan, A.D. Jeyasekharan, ROS and the DNA damage response in cancer, Redox Biol. 25 (2019), 101084, https://doi.org/10.1016/j.redox.2018.101084.
[75] A. Lezaja, M. Altmeyer, Inherited DNA lesions determine G1 duration in the next cell cycle, Cell Cycle. 17 (2018) 24–32, https://doi.org/10.1080/15384101.2017.1383578.
[76] F. Ito, Y. Sono, T. Ito, Measurement and Clinical Significance of Lipid Peroxidation as a Biomarker of Oxidative Stress: Oxidative Stress in Diabetes, Atherosclerosis, and Chronic Inflammation, Antioxidants. 8 (2019) 72, https://doi.org/10.3390/antiox8030072.
[77] R. Canaparo, F. Foglietta, N. Barbero, L. Serpe, The promising interplay between sonodynamic therapy and nanomedicine, Adv Drug Deliv Rev. 189 (2022), 114495, https://doi.org/10.1016/j.addr.2022.114495.
[78] S.M. Burrow, D.A. Phoenix, M. Wainwright, M.J. Tobin, Intracellular localisation studies of doxorubicin and Victoria Blue BO in EMT6-S and EMT6-R cells using confocal microscopy, Cytotechnology. 39 (2002) 15–25, https://doi.org/10.1023/A:1022435829894.
[79] S.R. Shaikh, M. Edidin, Polyunsaturated fatty acids and membrane organization: elucidating mechanisms to balance immunotherapy and susceptibility to infection, Chem Phys Lipids. 153 (2008) 24–33, https://doi.org/10.1016/j.chemphyslip.2008.02.008.
[80] X. Wang, H. Fang, Z. Huang, W. Shang, T. Hou, A. Cheng, H. Cheng, Imaging ROS signaling in cells and animals, J Mol Med. 91 (2013) 917–927, https://doi.org/10.1007/s00109-013-1067-4.
[81] Y.N. Korystov, V. v. Shaposhnikova, A.F. Korystova, M.O. Emel'yanov, Detection of Reactive Oxygen Species Induced by Radiation in Cells Using the Dichlorofluorescein Assay, Radiat Res. 168 (2007) 226–232. https://doi.org/10.1667/RR0925.1.
[82] F.-Y. Huang, J. Lei, Y. Sun, F. Yan, B. Chen, L. Zhang, Z. Lu, R. Cao, Y.-Y. Lin, C.-C. Wang, G.-H. Tan, Induction of enhanced immunogenic cell death through ultrasound-controlled release of doxorubicin by liposome-microbubble complexes, Oncoimmunology. 7 (2018) e1446720.
[83] C. Donohoe, M.O. Senge, L.G. Arnaut, L.C. Gomes-da-Silva, Cell death in photodynamic therapy: From oxidative stress to anti-tumor immunity, Biochimica et Biophysica Acta (BBA) - Reviews on, Cancer. 1872 (2019), 188308, https://doi.org/10.1016/j.bbcan.2019.07.003.